Haproff, P.J., Levy, D.A., Zuza, A.V., Hooker, J.D., Heizler, M.T., Stockli, D.F., and Braza, M., 2022, Cenozoic kinematic histories of the Tidding and Lohit thrusts in the northern Indo-Burma Ranges: Implications for crustal thickening and exhumation of Gangdese lower arc crust along the Indus-Yarlung suture zone: GSA Bulletin, https://doi.org/10.1130/B36323.1.

SUPPLEMENTARY MATERIAL

Description of $^{40}Ar/^{39}Ar$ thermochronology procedure for samples PH-1-8-13-22B, PH-11-9-15-36, PH-11-10-15-19, and PH-1-15-20-6.

Mineral separation and $^{40}Ar/^{39}Ar$ analyses were performed at the Nevada Isotope Geochronology Lab, University of Nevada, Las Vegas. Prior to analysis, muscovite separates were wrapped in Al foil and stacked in sealed and fused silica tubes of 6-mm inside diameter. Individual packets of muscovite grains averaged 2 mm in thickness. Neutron fluence monitors (GA-1550 biotite) were placed every 5–10 mm along the silica tubes. Synthetic K-glass and optical-grade CaF_2 were included in the irradiation packages to monitor neutron-induced Ar interferences from K and Ca. Loaded silica tubes were packed in an Al container for irradiation at the Oregon State TRIGA Reactor in Corvallis, OR. Loaded silica tubes were in-core for 26 hours in the F-12 position, In-Core Irradiation Tube of the 1 MW TRIGA-type reactor.

Correction factors for interfering neutron reactions on K and Ca were determined by repeated analysis of K-glass and CaF_2 fragments. Measured $(^{40}Ar/^{39}Ar)_K$ values were 1.07 (± 6.30%) x 10^{-2}. Ca correction factors were $(^{36}Ar/^{37}Ar)_{Ca}$ = 2.31 (± 0.25%) x 10^{-4} and $(^{39}Ar/^{37}Ar)_{Ca}$ = 6.55 (± 0.20%) x 10^{-4}. J factors were determined by fusion of 6–10 individual crystals of neutron fluence monitors which provided 0.09% to 0.11% reproducibility at each standard position. The curve fit function in the program MATLAB was used to determine J and uncertainty in J at each standard position. No significant neutron fluence gradients were present within individual packets of crystals as indicated by the reproducibility of the single crystal fluence monitor fusions.

Irradiated FC-2 sanidine standards and CaF_2 and K-glass fragments were placed in a Cu sample tray in a high vacuum extraction line and fused using a 20 W CO_2 laser. Sample viewing during laser fusion was performed via video camera system. Sample positioning was performed using a motorized sample stage. Samples analyzed by the furnace step heating method utilized a double vacuum resistance furnace using the design of Staudacher et al. (1978). Reactive gases were removed by three GP-50 SAES getters prior to being admitted to a MAP 215-50 mass spectrometer by expansion. The relative volumes of the extraction line and mass spectrometer allow 80% of the gas to be admitted to the mass spectrometer for laser fusion analyses and 76% for furnace heating analyses. Peak intensities were measured using a Balzers electron multiplier by peak hopping through seven cycles. Initial peak heights were determined by linear regression to the time of gas admission. Mass spectrometer discrimination and sensitivity were monitored by repeated analysis of atmospheric Ar aliquots from an on-line pipette system. Measured $^{40}Ar/^{36}Ar$ ratios were 282.82 ± 0.03% during this procedure. A discrimination correction of 1.0448 (4 AMU) was applied to measured isotope ratios. The sensitivity of the mass spectrometer was ~6 x 10^{-17} mol mV^{-1}. The multiplier operated at a gain of 36 over the Faraday. During laser fusion analyses, line blanks averaged 2.90 mV and 0.02 mV for mass 40 and 36, respectively. For furnace heating analyses, line blanks averaged 72.62 mV and 0.25 mV for mass 40 and 36, respectively. Discrimination, sensitivity, and blanks were relatively constant over the

period of data collection. Computer automated operation of the sample stage, laser, extraction line, mass spectrometer operation, and final data reduction and age calculations were performed using LabSPEC software written by B. Idleman (Lehigh University). An age of 98.50 Ma (Spell and McDougall, 2003) was used for the GA-1550 biotite fluence monitor in calculating ages for samples.

In the $^{40}Ar/^{39}Ar$ results, individual plateau step segments consist of three or more contiguous gas fractions that have analytically indistinguishable ages (i.e., all plateau steps overlap in age at $\pm$ 2σ analytical error). All individual step ages are reported at the confidence level of 1σ (standard deviation). Weighted mean ages of similar-aged individual step segments were calculated using the online program IsoplotR (Vermeesch, 2018).

References

Spell, T.L., McDougall, I., 2003, Characterization and calibration of $^{40}Ar/^{39}Ar$ dating standards: Chemical Geology, v. 198, p. 189-211.

Staudacher, T.H., Jessberger, E.K., Dorflinger, D., Kiko, J., 1978, A refined ultrahigh-vacuum furnace for rare gas analysis: J. Phys. E: Sci. Instrum., v. 11, p. 781-784.

Vermeesch, P., 2018, IsoplotR: a free and open toolbox for geochronology: Geoscience Frontiers, v.9, p.1479-1493, doi: 10.1016/j.gsf.2018.04.001.

Description of multi-domain diffusion $^{40}Ar/^{39}Ar$ thermochronology procedure for sample PH-11-11-15-14.

Multi-diffusion domain (MDD) thermal histories were obtained using the basic procedures of Lovera et al. (1989), Sanders et al. (2006), and Long et al. (2018). For MDD modeling, diffusion coefficients are calculated based on the fractional release of ^{39}Ar and plotted on the Arrhenius plots. Log(r/r_0) plots were obtained using an activation energy of 46 kcal/mol for K-feldspar (Lovera et al., 1997) using the convention of placing the reference Arrhenius law (r_0) to pass through the first heating step such that the log(r/r_0) value is zero for the first increment of gas release. The Arrhenius data were forward modeled with equal activation energy for each domain and yield model fits that closely match the measured data. Thermal histories are determined by fitting the measured age spectrum with acceptable fits determined by a Chebyshev's approximation. A minimum of twenty successful model fits is used to determine a mean and 90% confidence interval for the thermal histories that only allow cooling from an initially high temperature. Additional details of the $^{40}Ar/^{39}Ar$ analysis and MDD modeling are provided in the supplementary tables.

References

Long, S.P., Heizler, M.T., Thomson, S.N., Reiners, P.W., and Fryxell, J.E., 2018, Rapid Oligocene to early Miocene extension along the Grant Range detachment system, Nevada, USA: Insights from multipart cooling histories of footwall rocks: Tectonics, v. 2037 37, no. 12, p. 4752-4779.

Lovera, O.M., Grove, M., Harrison, T.M., 1997, Systematic analysis of K-feldspar $^{40}Ar/^{39}Ar$ step heating results; I, Significance of activation energy determination: Geochimica et Cosmochimica Acta, v. 61, no. 15, p. 3171-3192.

Lovera, O.M., Richter, F.M., and Harrison, T.M., 1989, The $^{40}Ar/^{39}Ar$ geothermometry for slowly cooled samples having a distribution of diffusion domain sizes: Journal of Geophysical Research, v. 94, no. 17, p. 917-17, 935.

Sanders, R.E., Heizler, M.T. and Goodwin, L.B., 2006, $^{40}Ar/^{39}Ar$ thermochronology constraints on the timing of Proterozoic basement exhumation and fault ancestry, southern Sangre de Cristo Range, New Mexico: Geological Society of America Bulletin, v. 118, no. 11, p. 1489-1506.

Description of microstructural and electron backscatter diffraction (EBSD) analytical procedure.

Oriented, whole-rock samples collected across the Lohit thrust shear zone were first cut parallel to the mineral stretching lineation and perpendicular to foliation to produce standard-sized (24x46 mm) petrographic thin sections by Wagner Petrographic Inc. in Lindon, UT. Thin sections were mounted with glass on one side and doubly polished to ~30-µm thickness. A second round of polishing was performed using a 0.25-µm abrasive. Mineral textures, microstructures, and kinematics were observed and imaged via optical microscopy at University of North Carolina Wilmington. Next, thin sections underwent a final ~8-hr vibratory polishing with 0.02-µm colloidal silica suspension to remove any remaining near-surface crystal lattice damage at University of Nevada, Reno (UNR).

EBSD analyses were performed using a Nordlys Nano high-resolution detector on a JEOL 7100 field emission scanning electron microscope at the Mackay Microbeam Laboratory, UNR. EBSD maps were generated by recording EBSD patterns from each node of a defined orthogonal grid. Preliminary EBSD maps were generated using ~10–30-µm step sizes. Higher-resolution EBSD maps were generated using ~5–12-µm step sizes. Postprocessing of EBSD data was performed using Oxford Instruments AZtecHKL 3.0 acquisition software (Cross et al., 2017). Run conditions for individual EBSD maps are listed in Table S6 below. Photomicrographs of samples used in EBSD analyses are shown in Supplemental Figures S11–15 below.

References

Cross, A.J., Prior, D.J., Stipp, M., and Kidder, S., 2017, The recrystallized grain size piezometer for quartz: An EBSD-based calibration: Geophysical Research Letters, v. 44, no. 13, p. 6667-6674.

Figure S1. Field photographs of leucogneiss and undeformed leucogranite dikes cross-cutting migmatitic orthogneiss of the Western Lohit Plutonic Complex Belt.

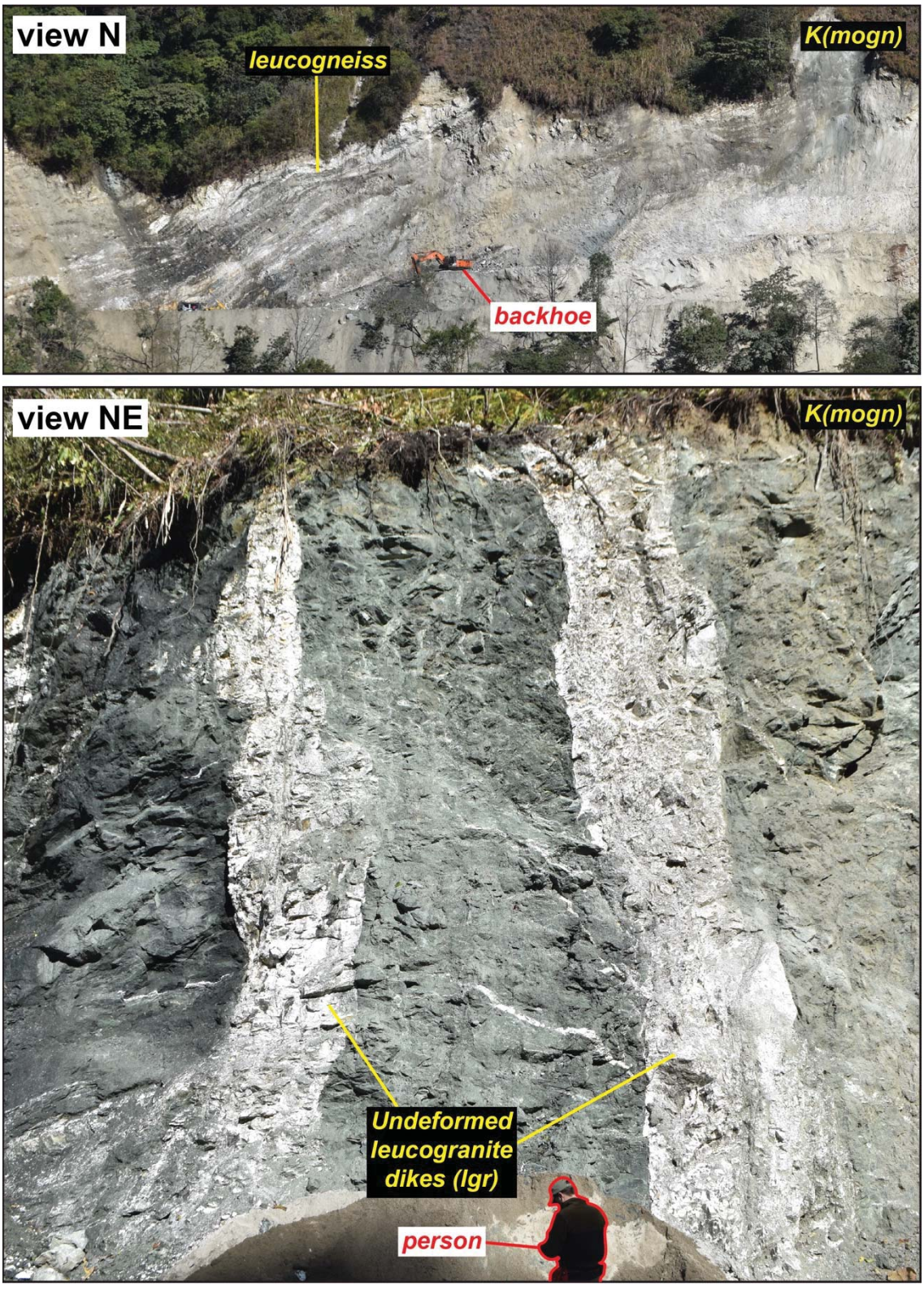

Figure S2. Field photographs of migmatitic orthogneiss of the Western Lohit Plutonic Complex Belt with interlayered felsic and mafic components that have been (A) folded and (B) cut by shear bands.

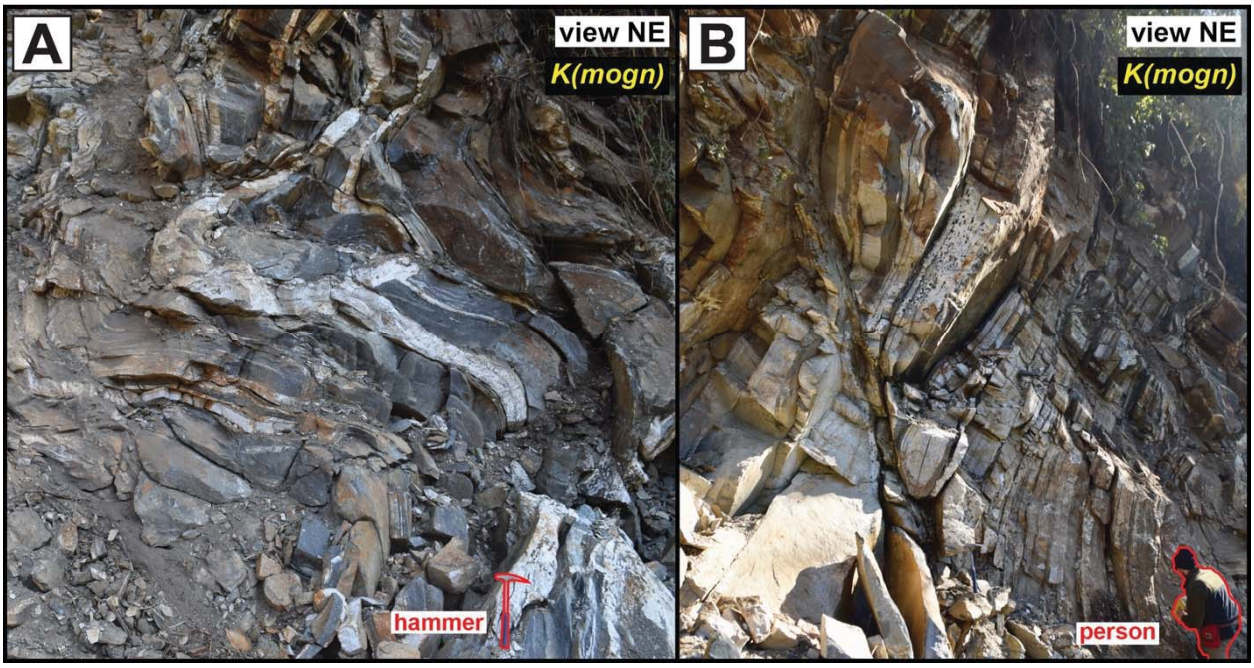

Figure S3. Field photographs of (A) the subvertical, southernmost section of the Lohit thrust shear zone within the Tidding mélange complex (footwall of the Lohit thrust fault), and (B-C) overturned to vertical, north-side-up asymmetric quartz boudins and isoclinal folds.

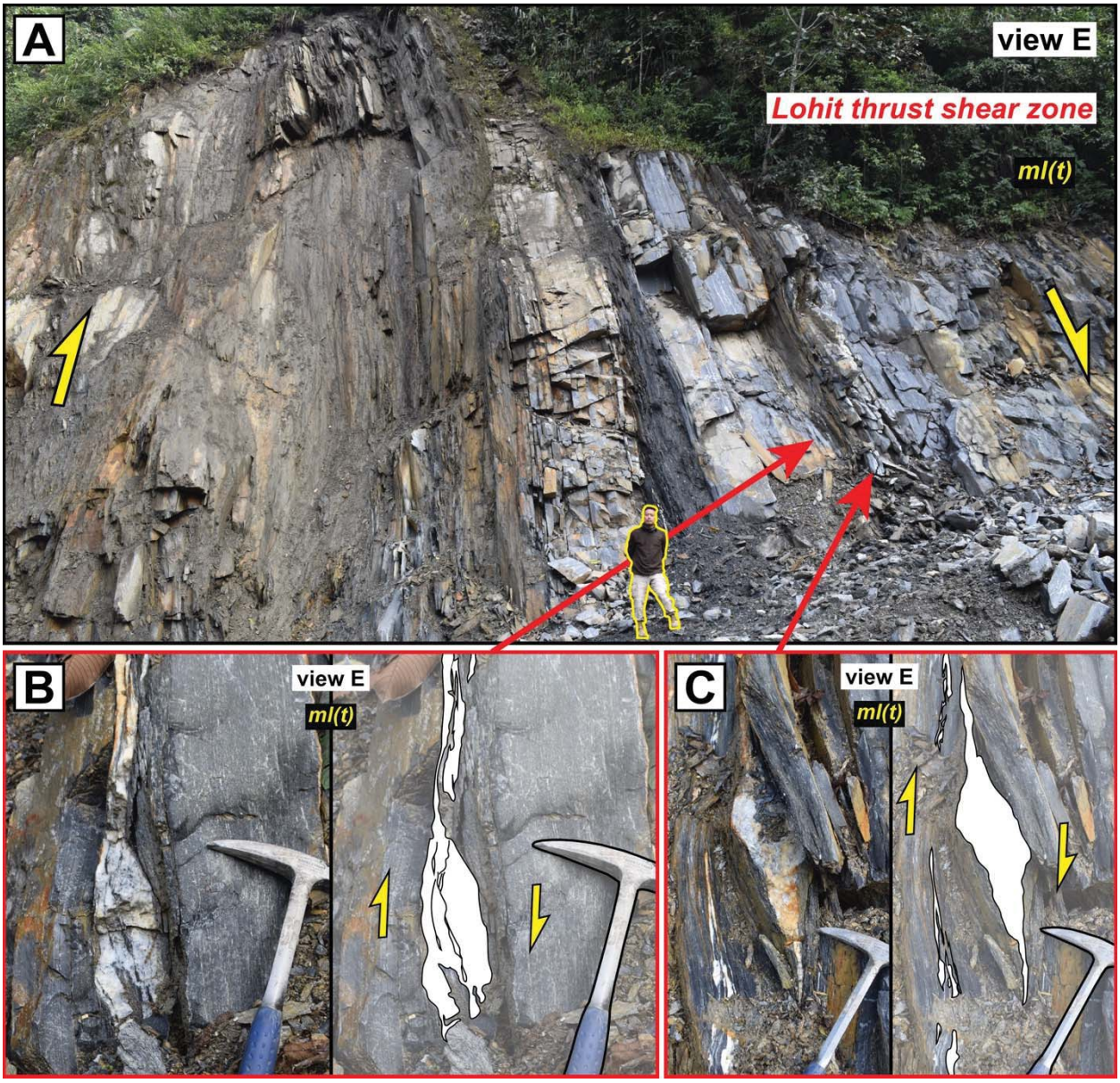

Figure S4. Field photograph of orthogneiss within the Lohit thrust shear zone containing subvertical foliation and north-side-up felsic boudin.

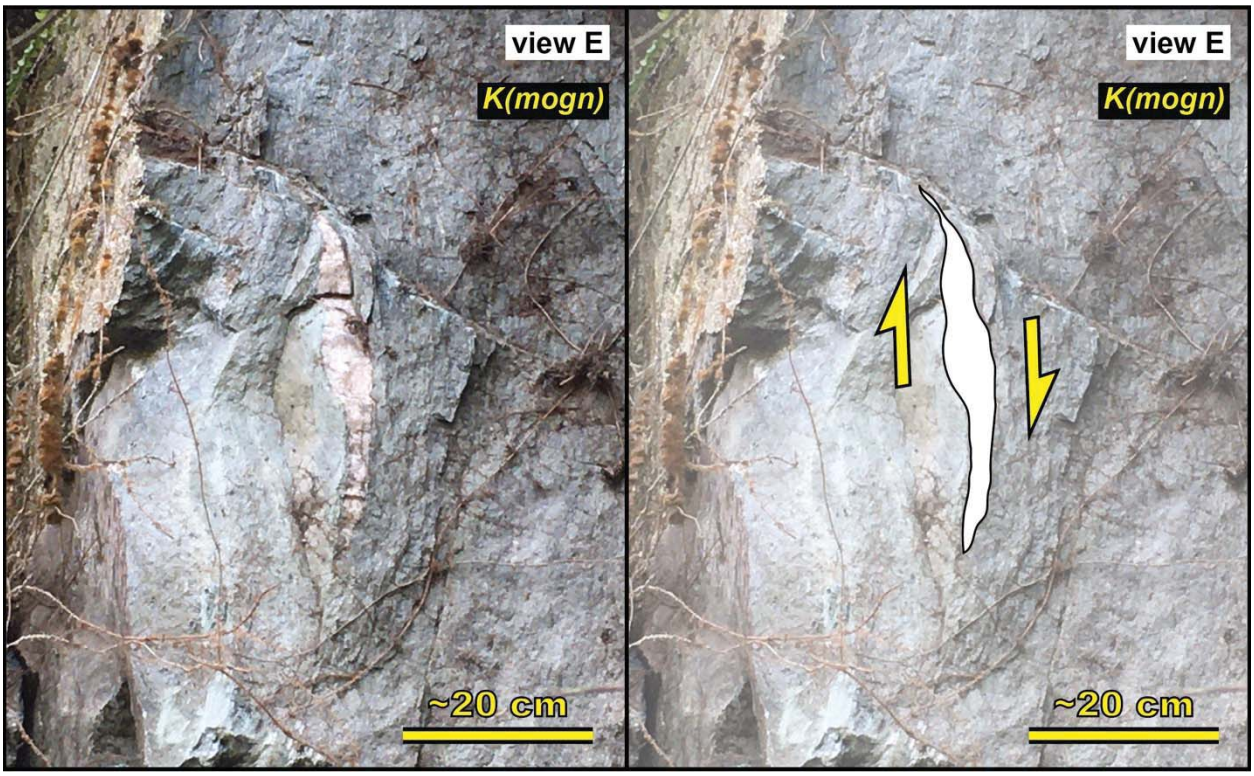

Figure S5. Cathodoluminescence images of representative zircons from leucogranite sample PH-1-14-20-9, collected from the Lohit thrust shear zone.

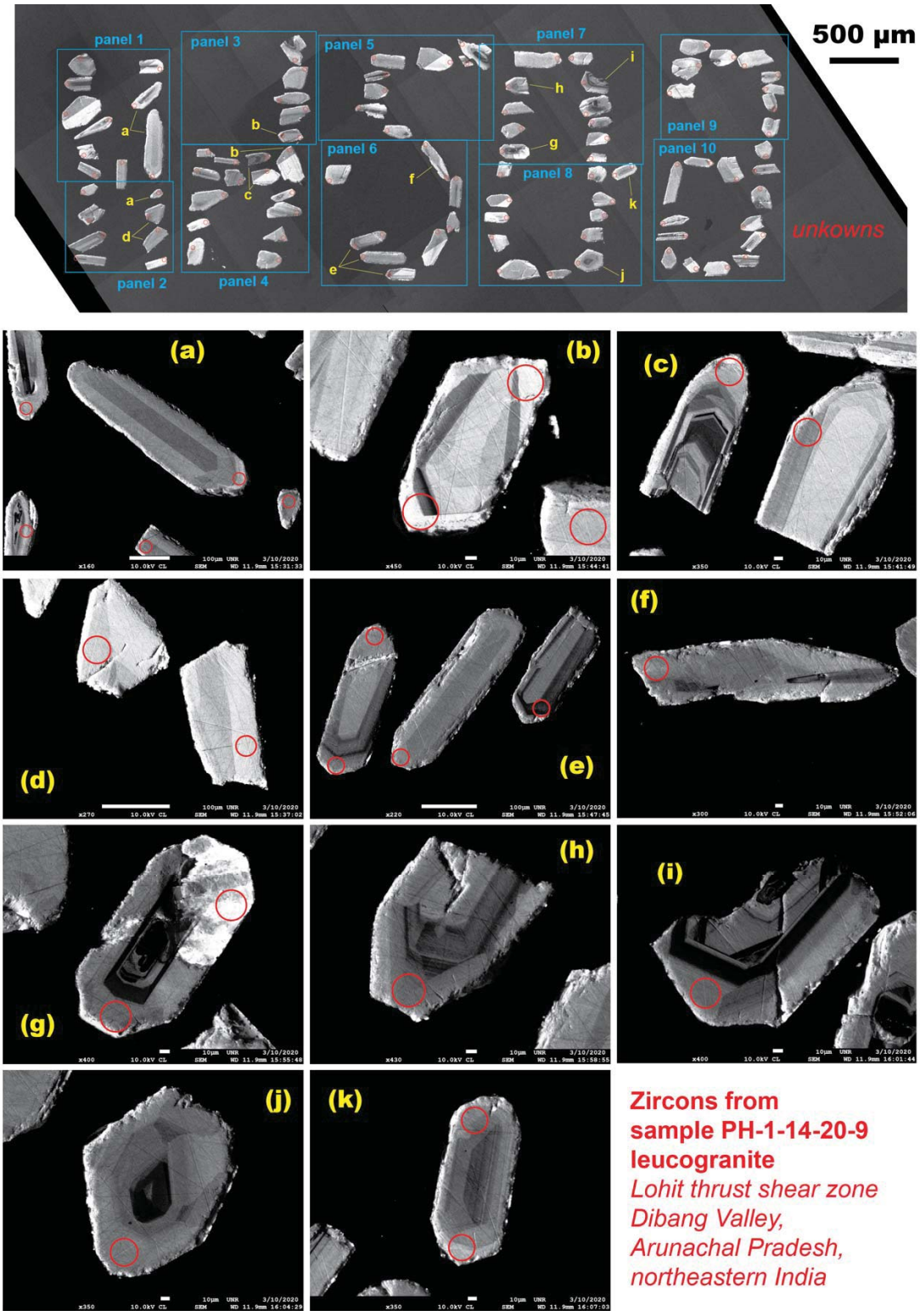

Figure S6. Total alkali versus silica plot of whole-rock Lohit Plutonic Complex samples from Dibang and Lohit Valleys, compiled from this study, Sharma et al. (1991), Goswami (2013), Lin et al. (2013), Haproff et al. (2019), Pebam and Kamalakannan (2019), and Bikramaditya et al. (2020).

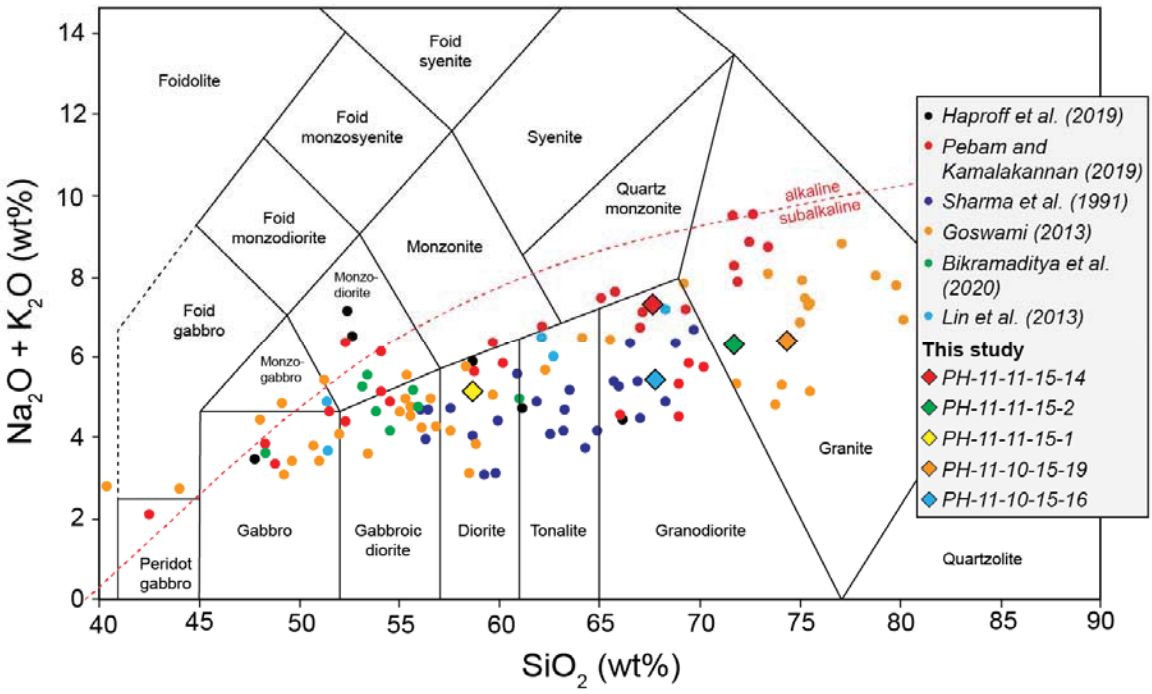

Figure S7. Whole-rock major and trace element geochemical plots of Lohit Plutonic Complex samples including (A) total alkali versus $Al_2O_3/(Na_2O + K_2O)$, (B) Rb versus Y + Nb, and (C) $Na_2O + K_2O$ versus 1000*Ga/Al, compiled from this study, Sharma et al. (1991), Goswami (2013), Lin et al. (2013), Haproff et al. (2019), Pebam and Kamalakannan (2019), and Bikramaditya et al. (2020).

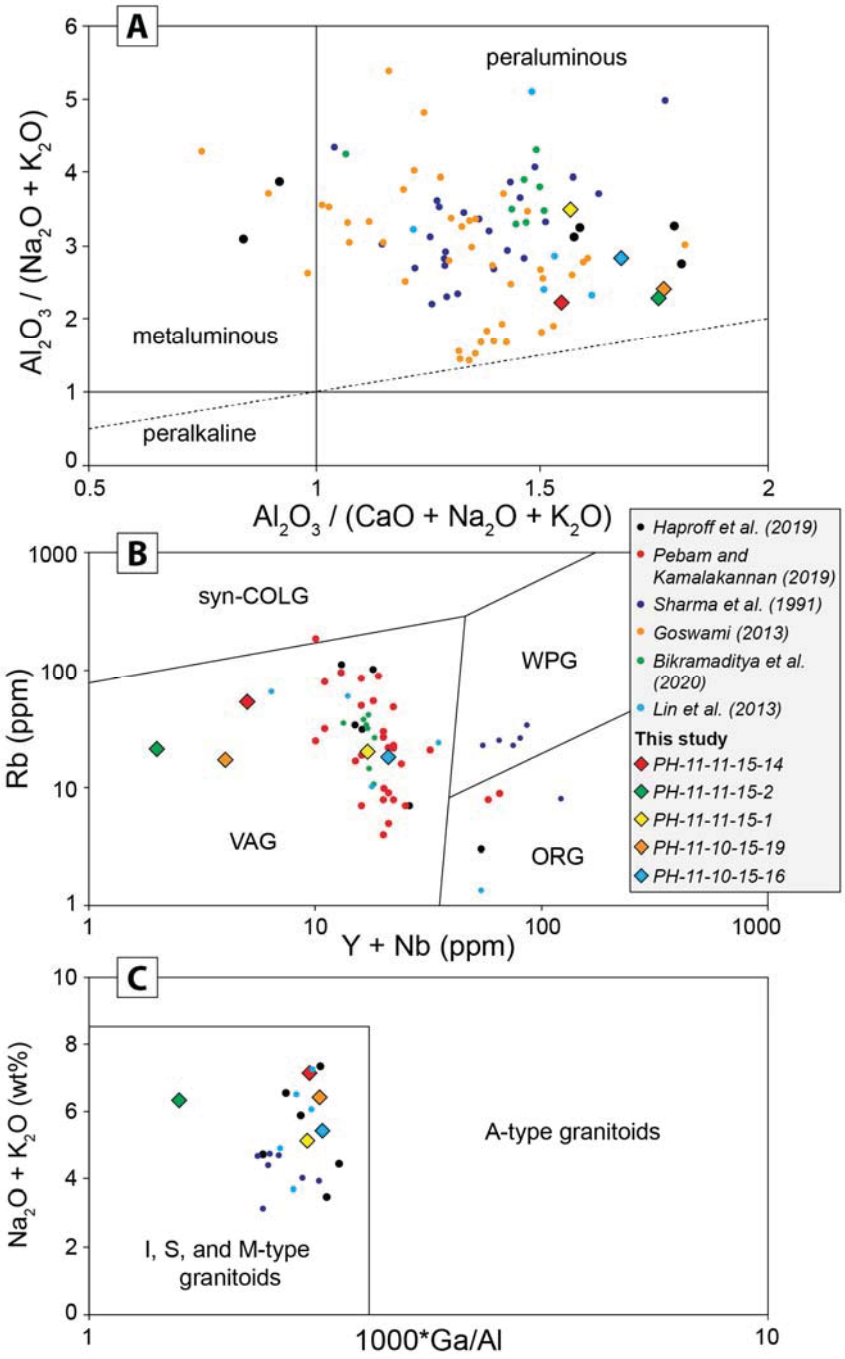

Figure S8. Plane-polarized (left) and cross-polarized-light (right) photomicrographs of sample PH-1-8-13-22B.

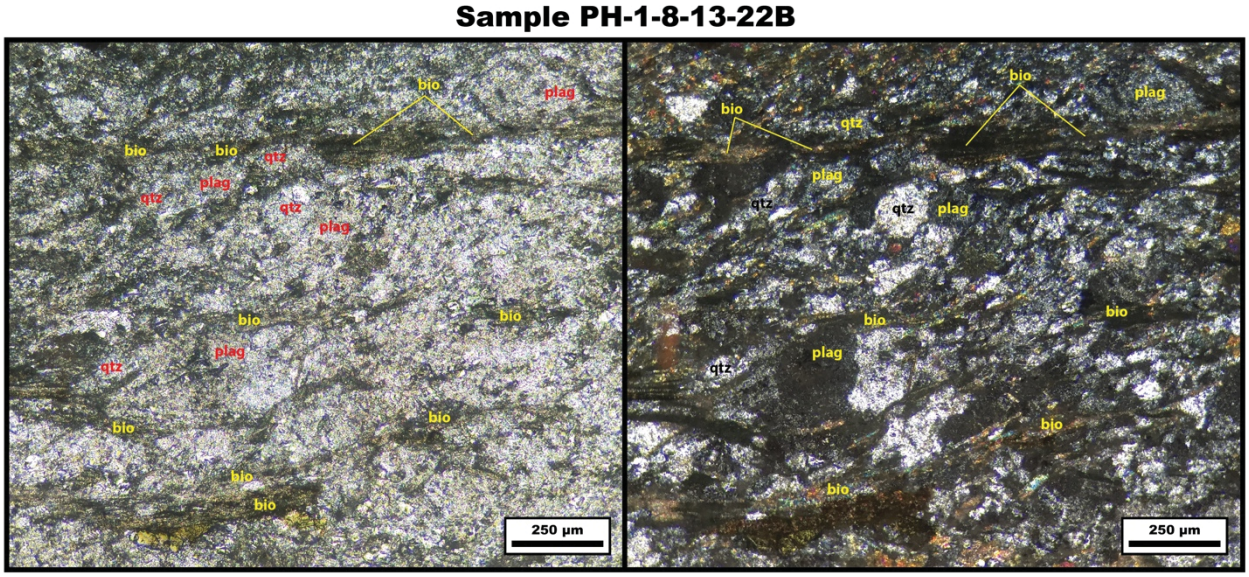

Figure S9. Plane-polarized (left) and cross-polarized-light (right) photomicrographs of sample PH-11-9-15-36.

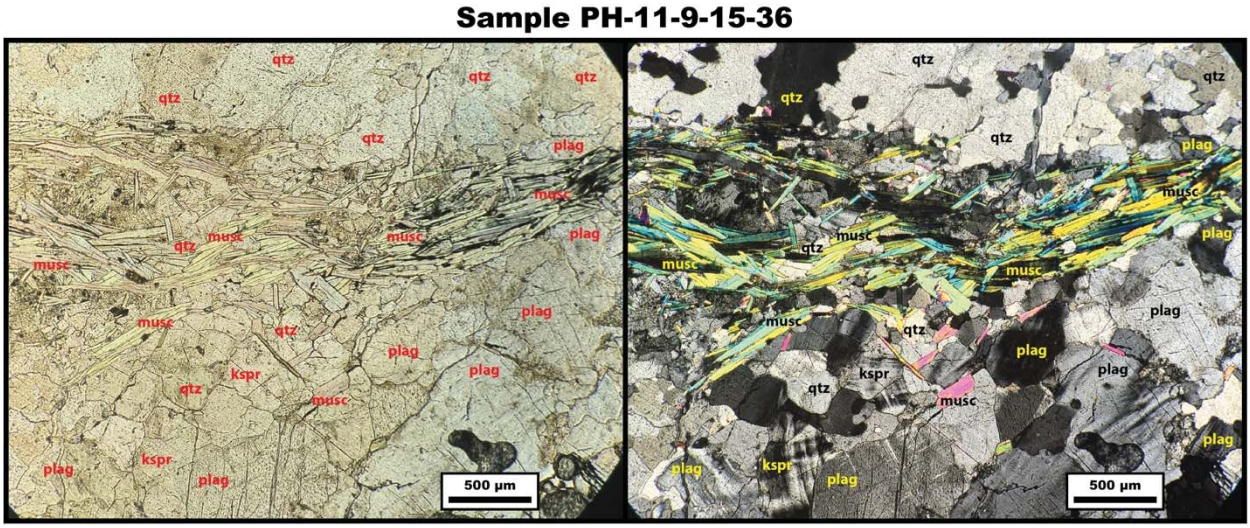

Figure S10. Plane-polarized (left) and cross-polarized-light (right) photomicrographs of sample PH-1-15-20-6.

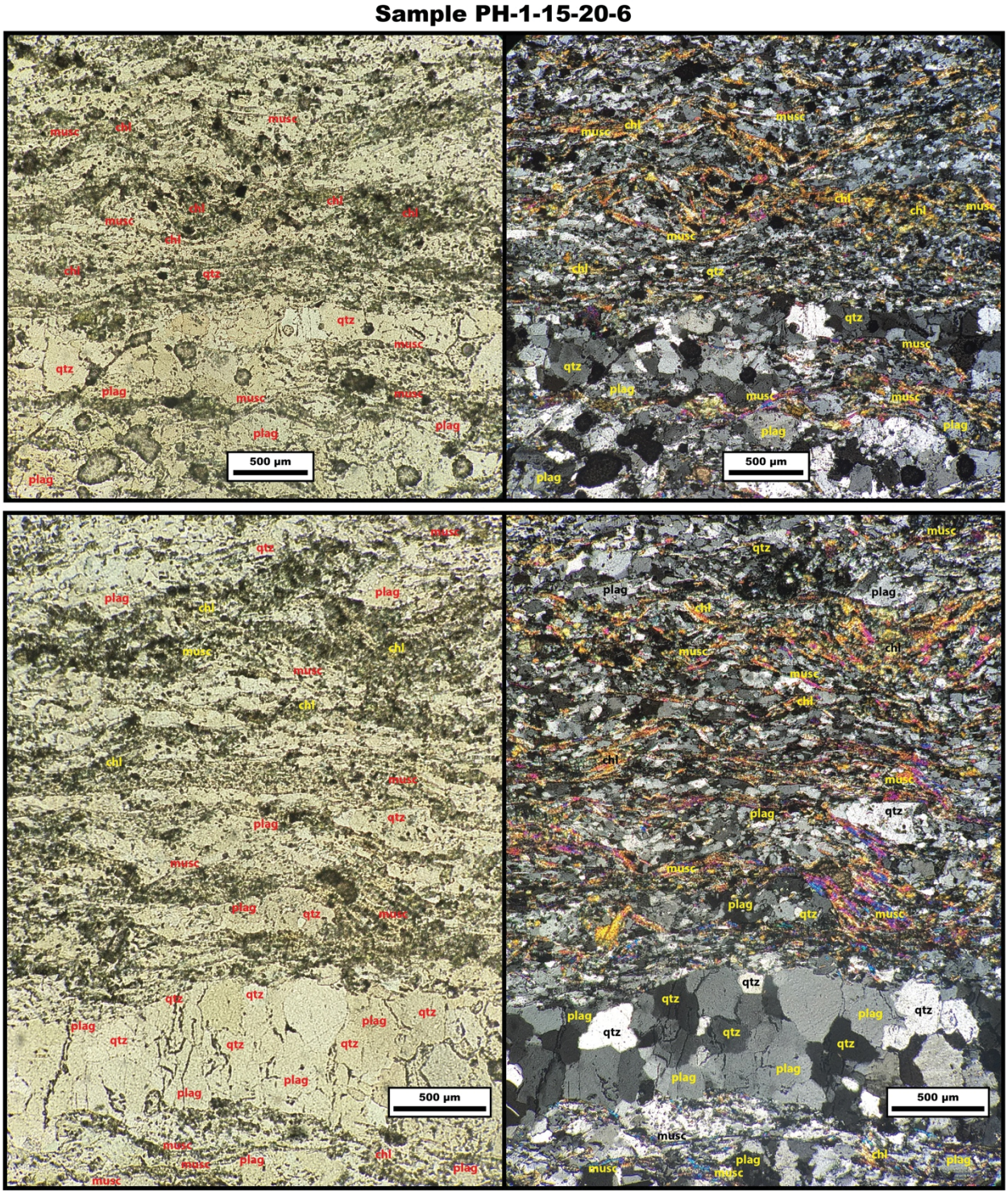

Figure S11. Plane-polarized (top and bottom left) and cross-polarized-light (top and bottom right) photomicrographs of sample PH-11-11-15-14. The middle photomicrographs are both in cross-polarized light.

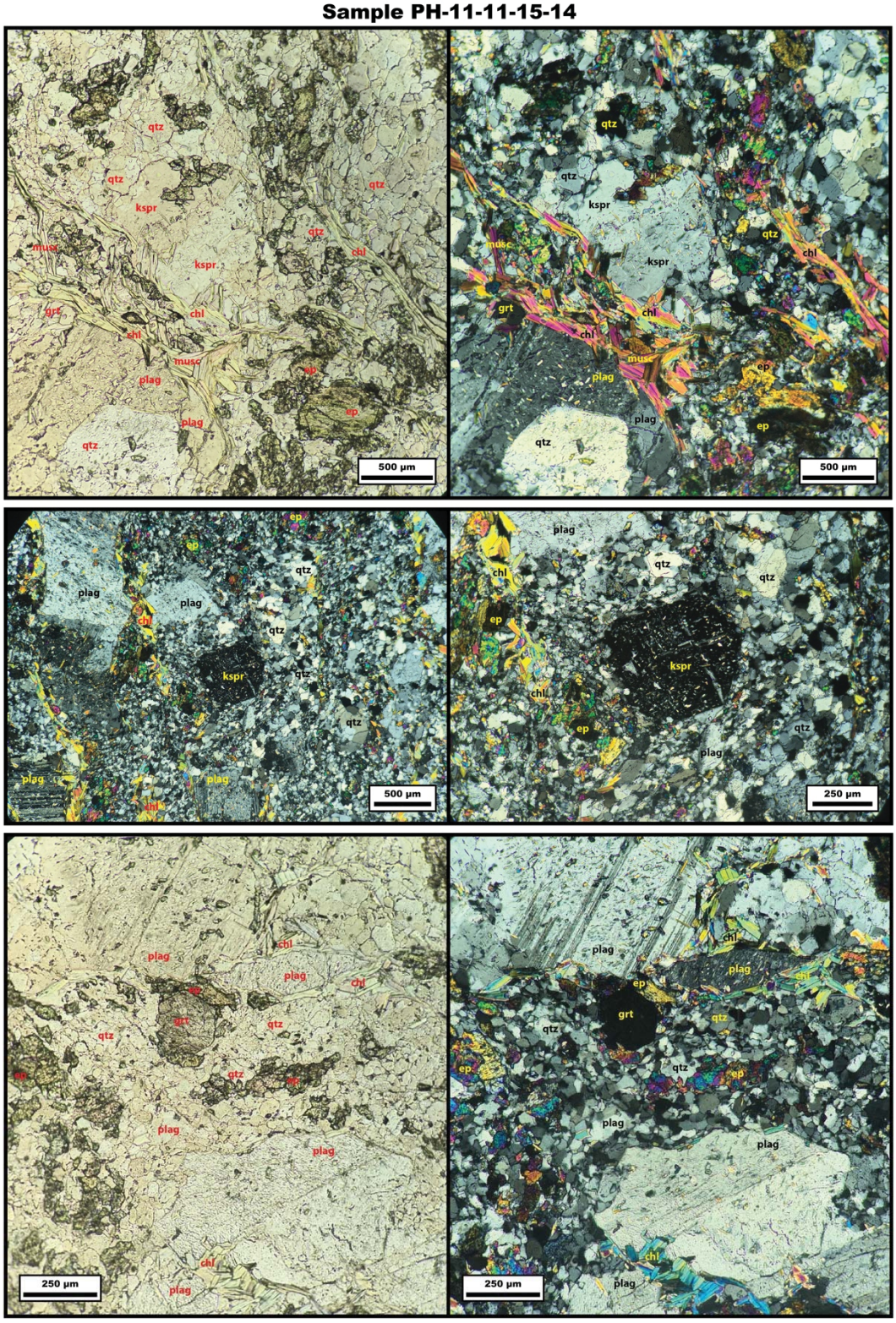

Figure S12. Potassium feldspar multi-diffusion domain $^{40}Ar/^{39}Ar$ thermochronology plots for sample PH-11-11-15-14 of the Lohit thrust shear zone, including Figures 11E and 11F of the main text (A and D, respectively).

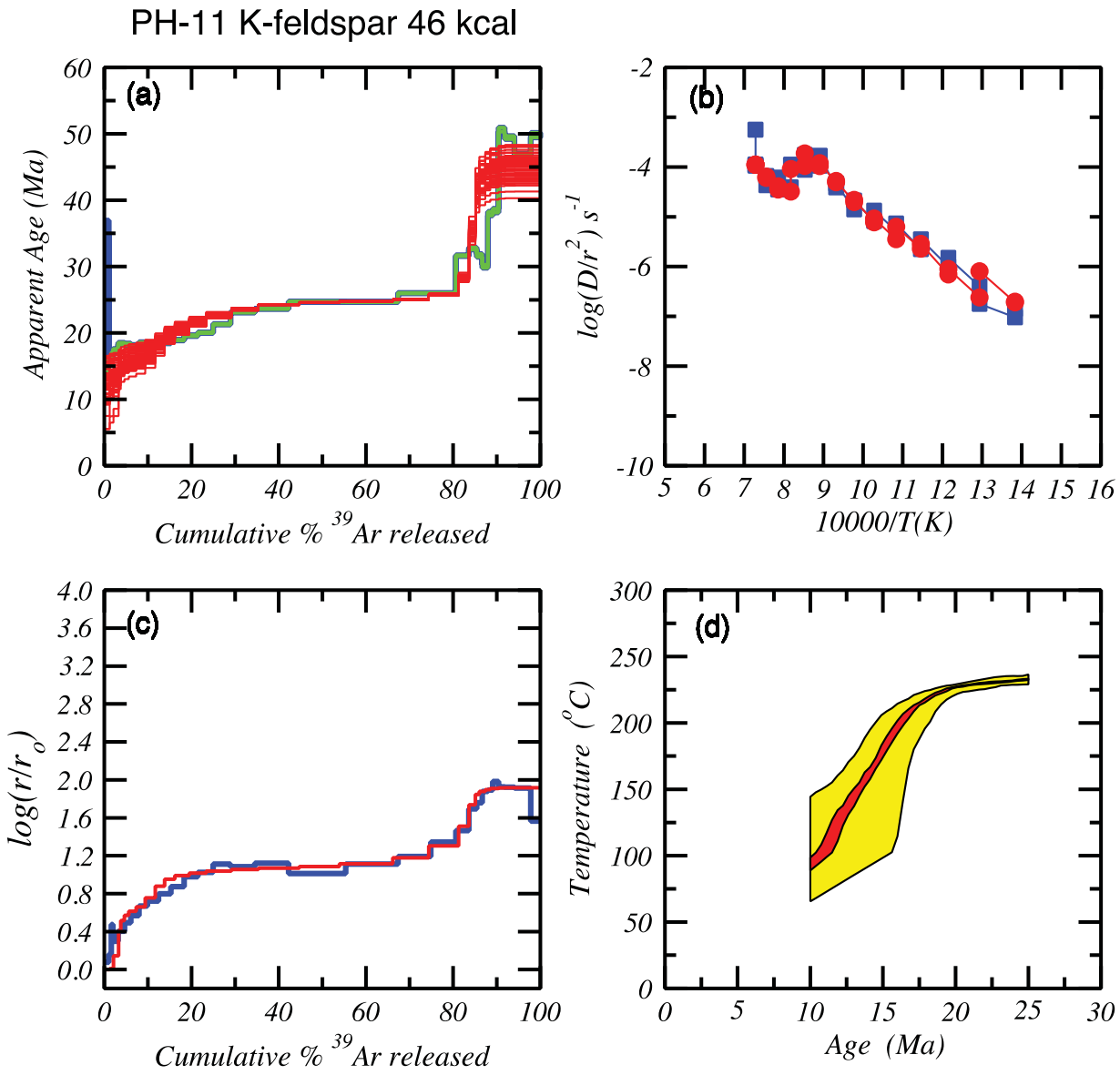

Figure S13. Plane-polarized (left) and cross-polarized-light (right) photomicrographs of sample PH-1-8-13-1B.

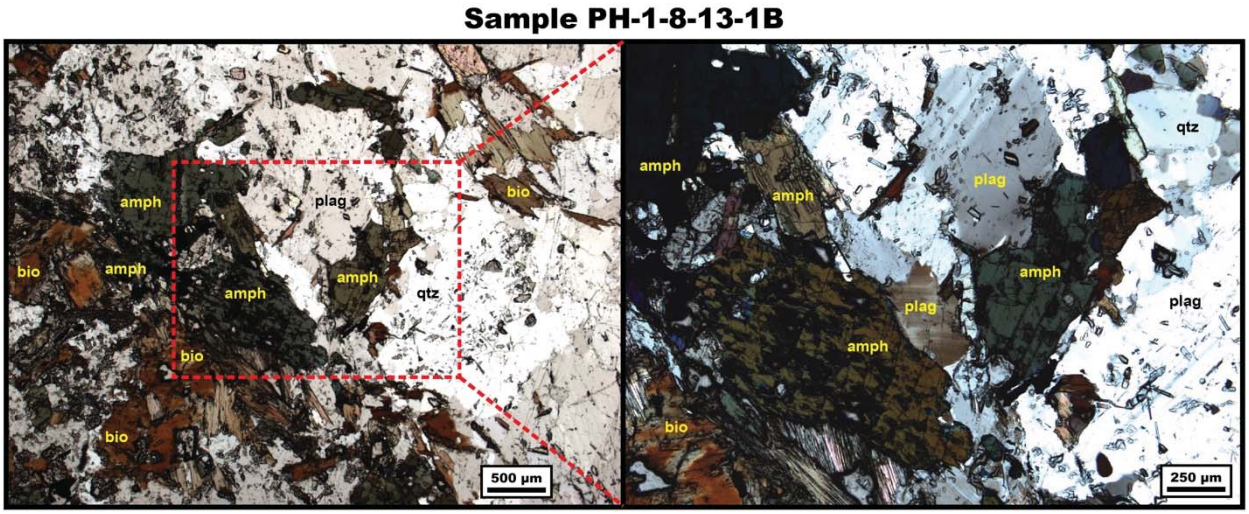

Figure S14. Plane-polarized (left) and cross-polarized-light (right) photomicrographs of sample PH-1-8-13-12A.

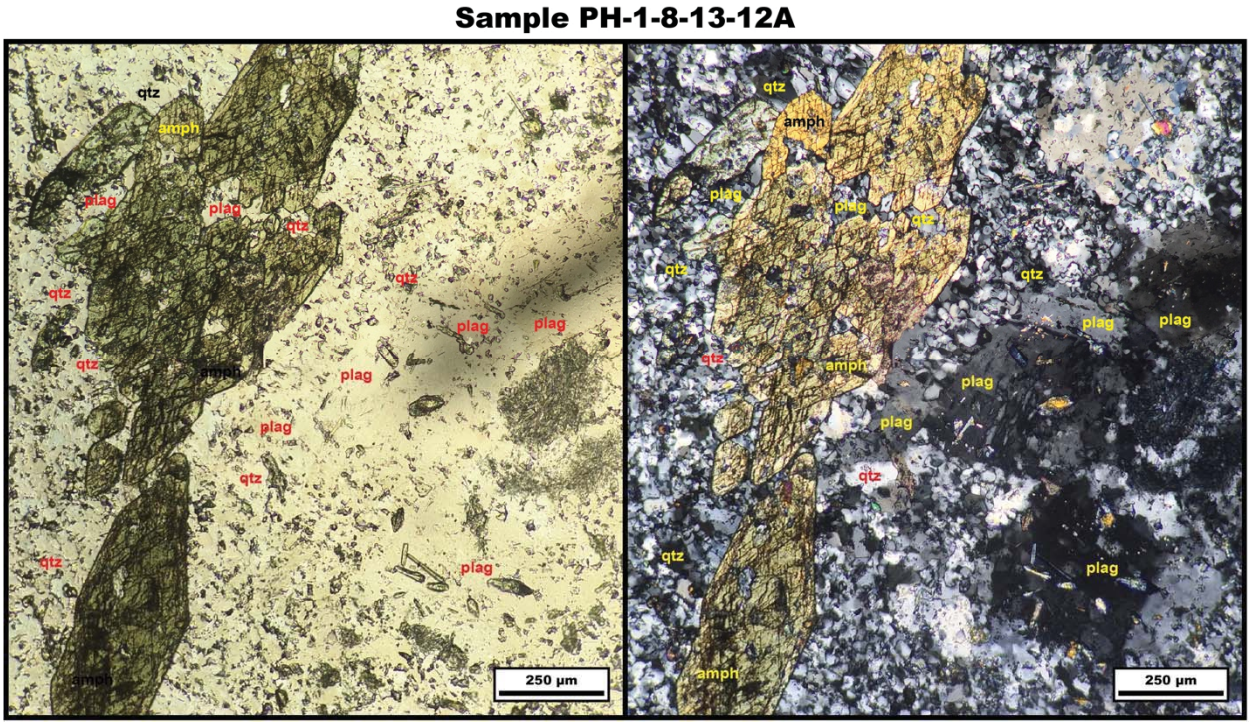

Figure S15. Plane-polarized (left) and cross-polarized-light (right) photomicrographs of sample AZ-11-10-15-6.

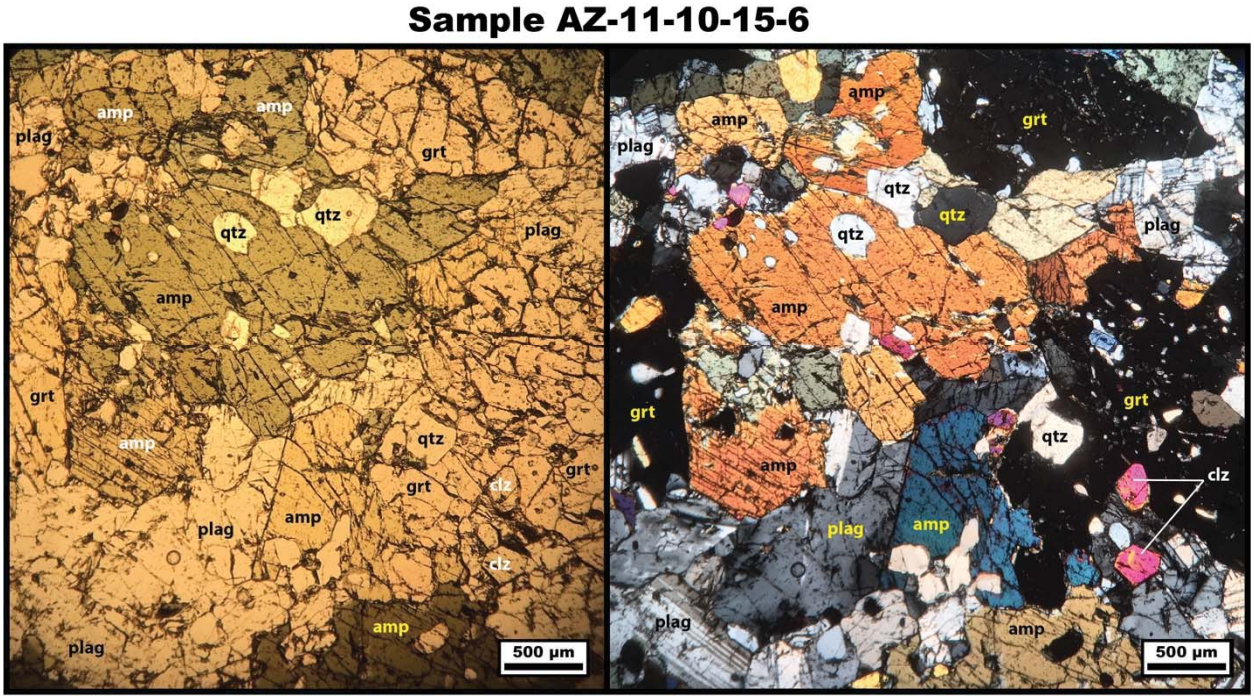

Figure S16. Electron microprobe garnet element traverses for geothermobarometry samples AZ-11-10-15-6, PH-11-12-15-17, and PH-1-9-13-8.

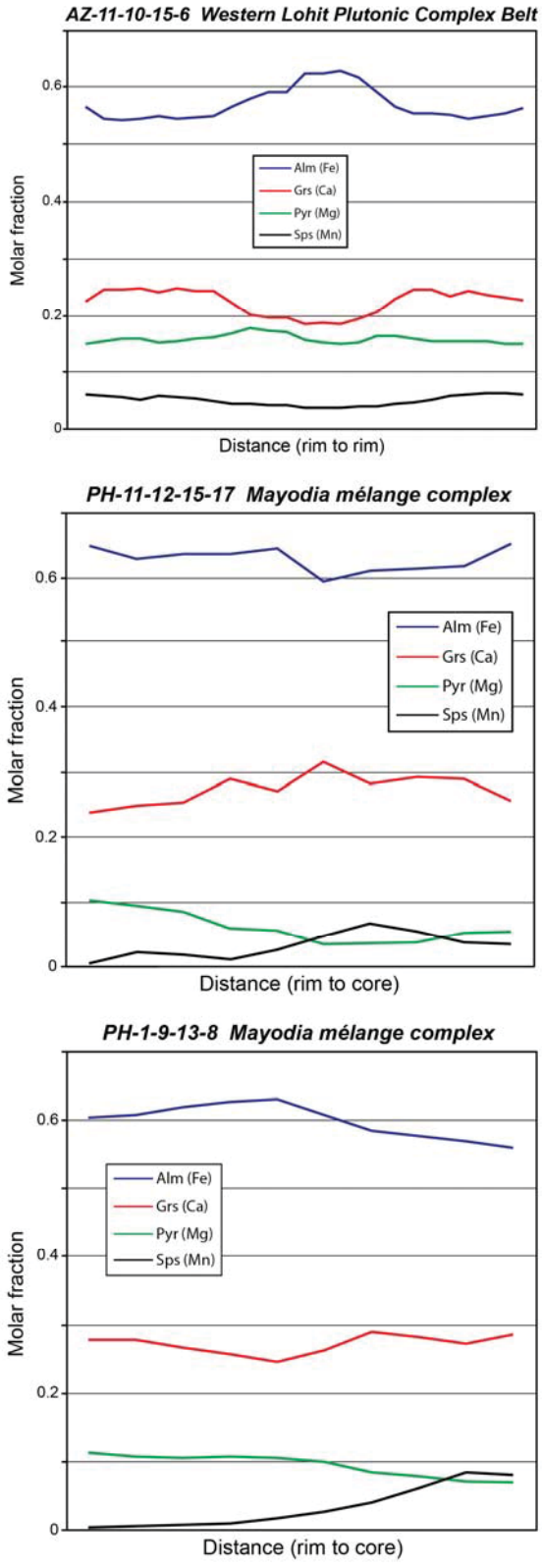

Figure S17. Plane-polarized (top and middle left) and cross-polarized-light (top and middle right) photomicrographs of sample PH-1-8-13-26. Both bottom photomicrographs are in cross-polarized light. The bottom left photomicrograph is adapted from Haproff et al. (2020).

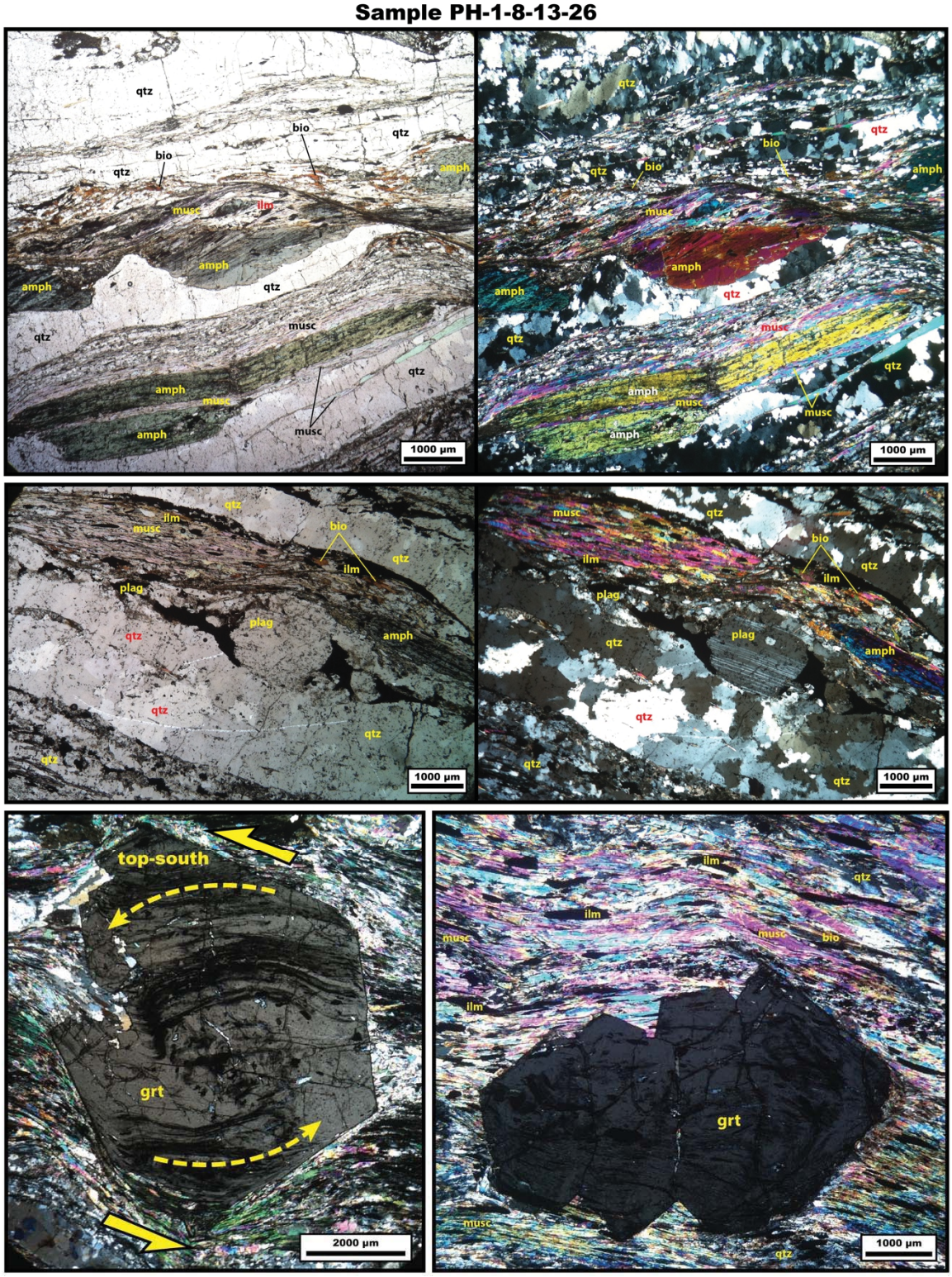

Figure S18. Plane-polarized (top and middle left) and cross-polarized-light (top and middle right and bottom) photomicrographs of sample PH-11-9-15-40.

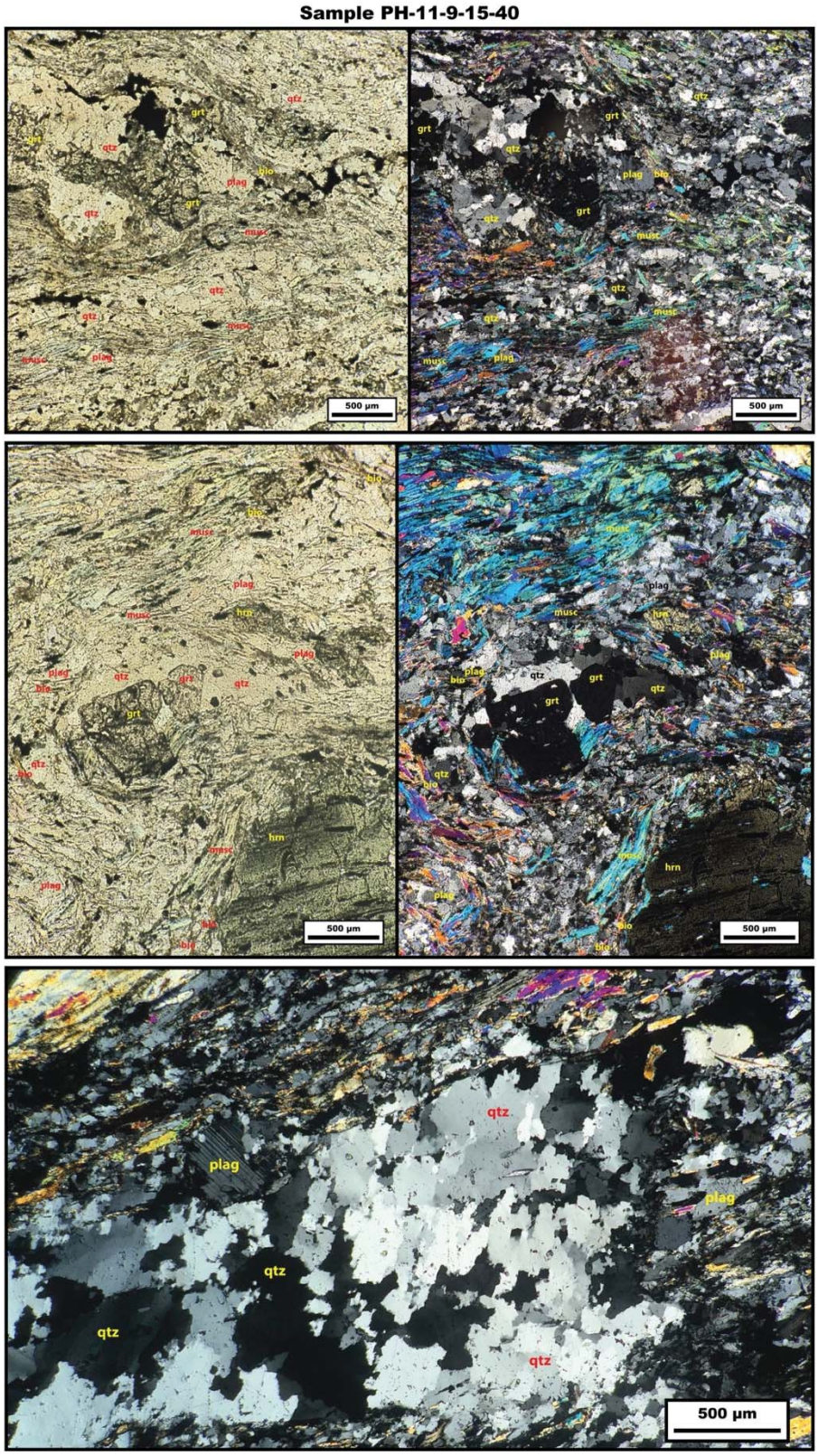

Figure S19. Plane-polarized (left) and cross-polarized-light (right) photomicrographs of sample PH-11-12-15-17.

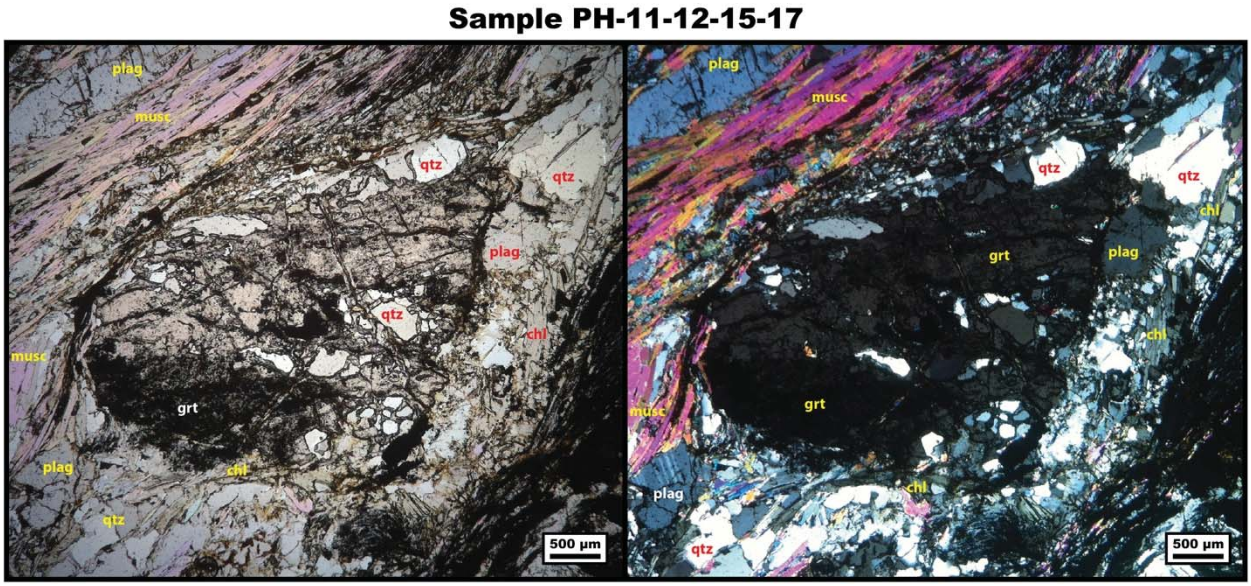

Figure S20. Plane-polarized (left) and cross-polarized-light (right) photomicrographs of sample PH-1-9-13-8.

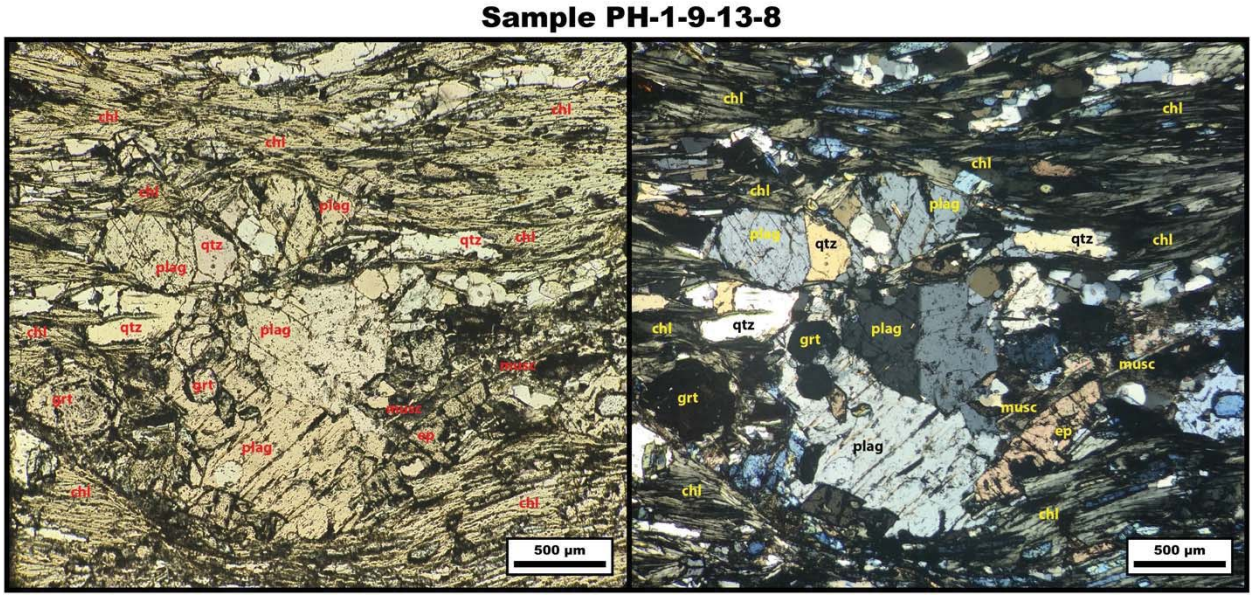

Figure S21. Electron microprobe garnet element map for sample PH-1-9-13-8.

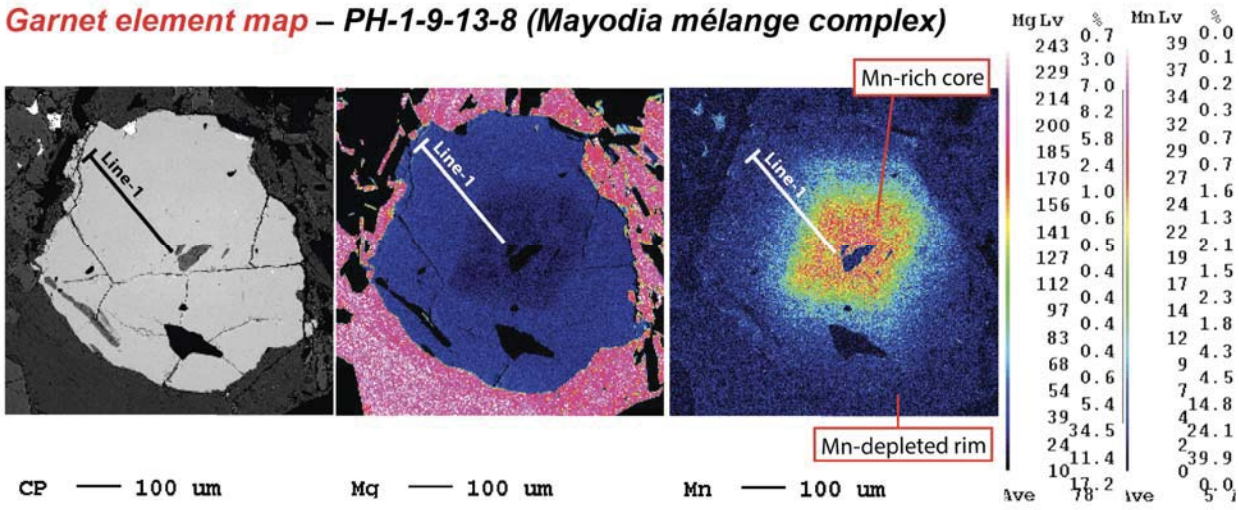

Figure S22. Plane-polarized (left) and cross-polarized-light (right) photomicrographs of EBSD sample PH-1-15-20-3.

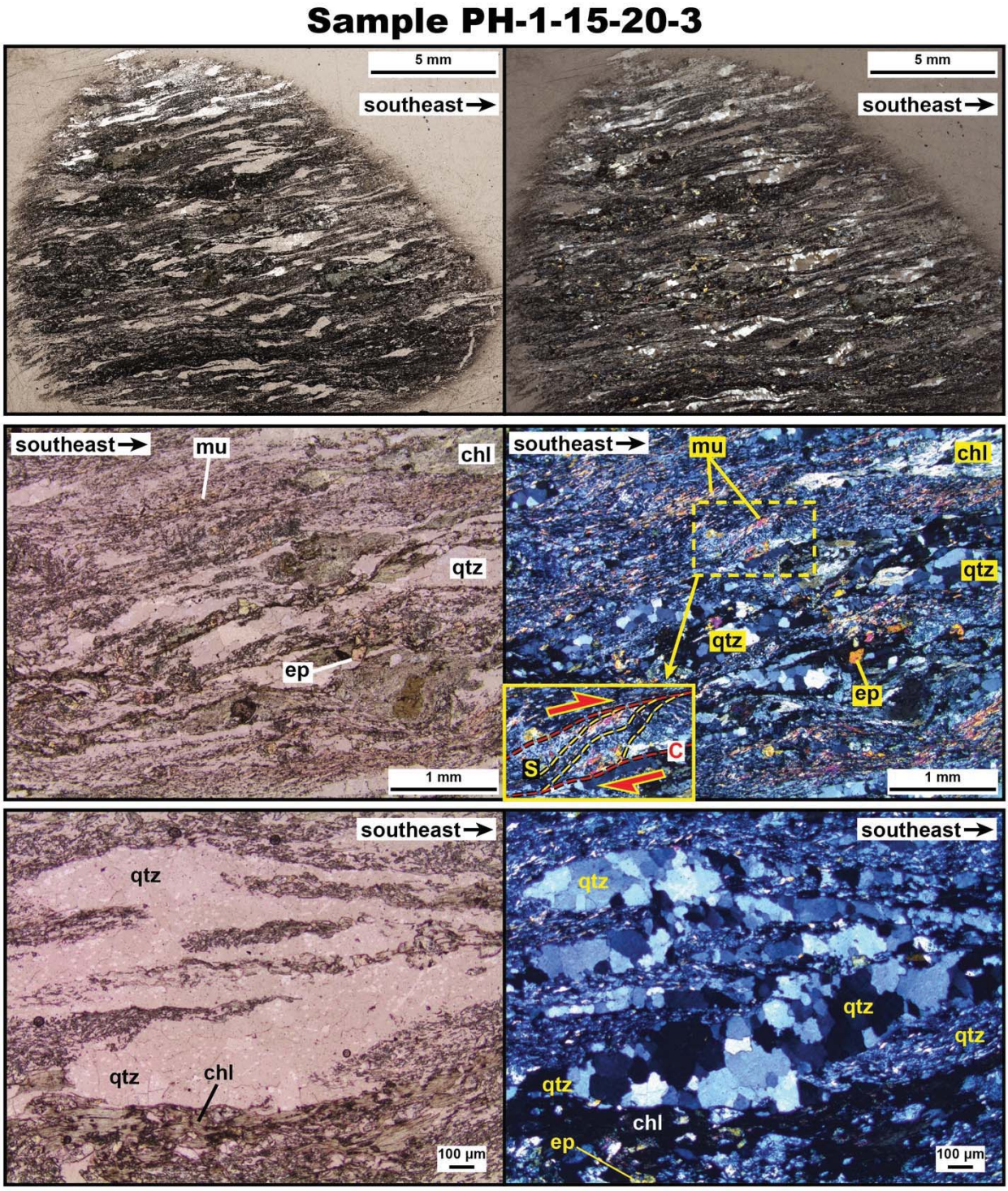

Figure S23. Plane-polarized (left) and cross-polarized-light (right) photomicrographs of EBSD sample PH-1-15-20-5.

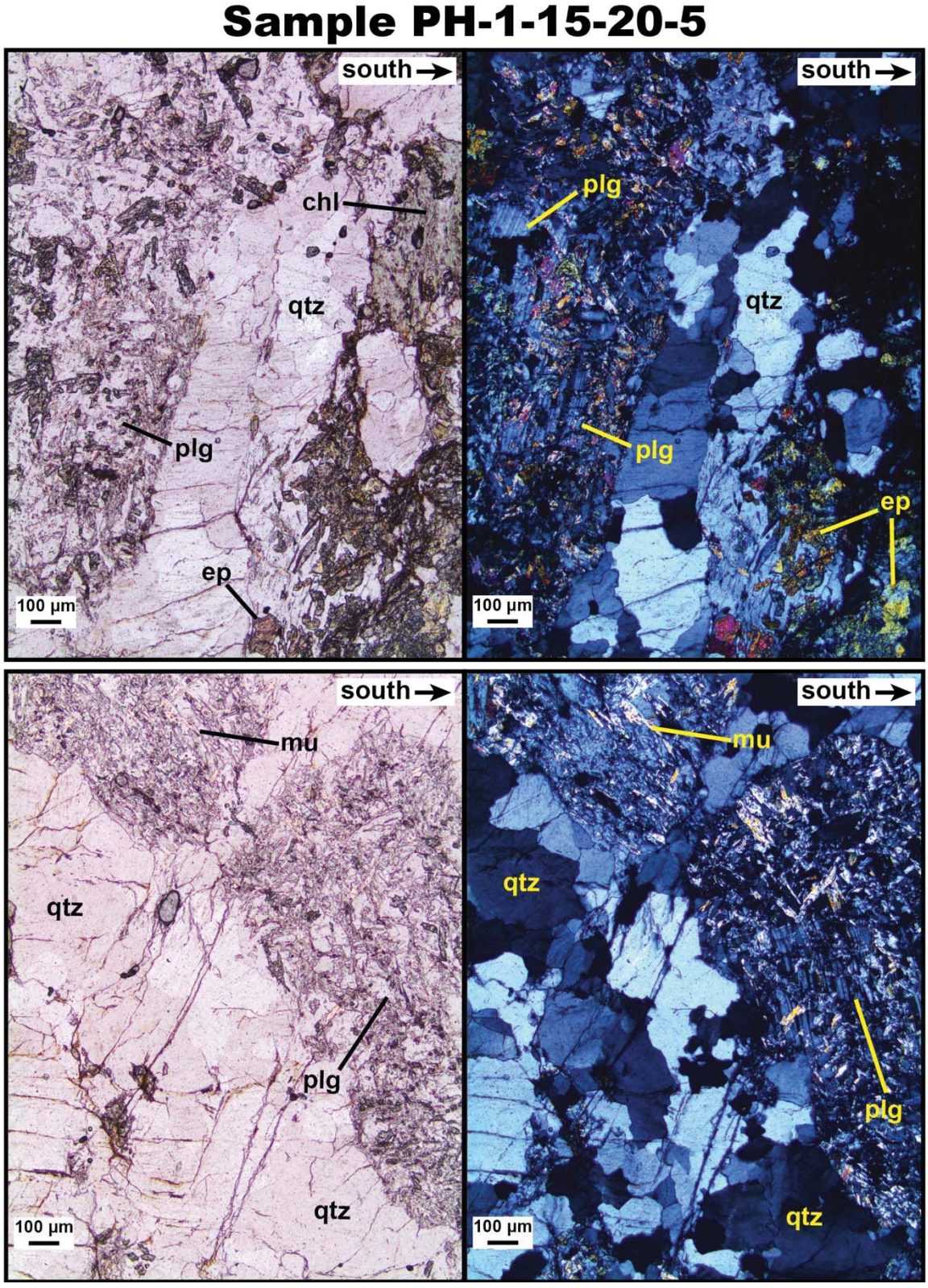

Figure S24. Plane-polarized (top and bottom left) and cross-polarized-light (bottom right) photomicrographs of EBSD sample PH-1-15-20-6.

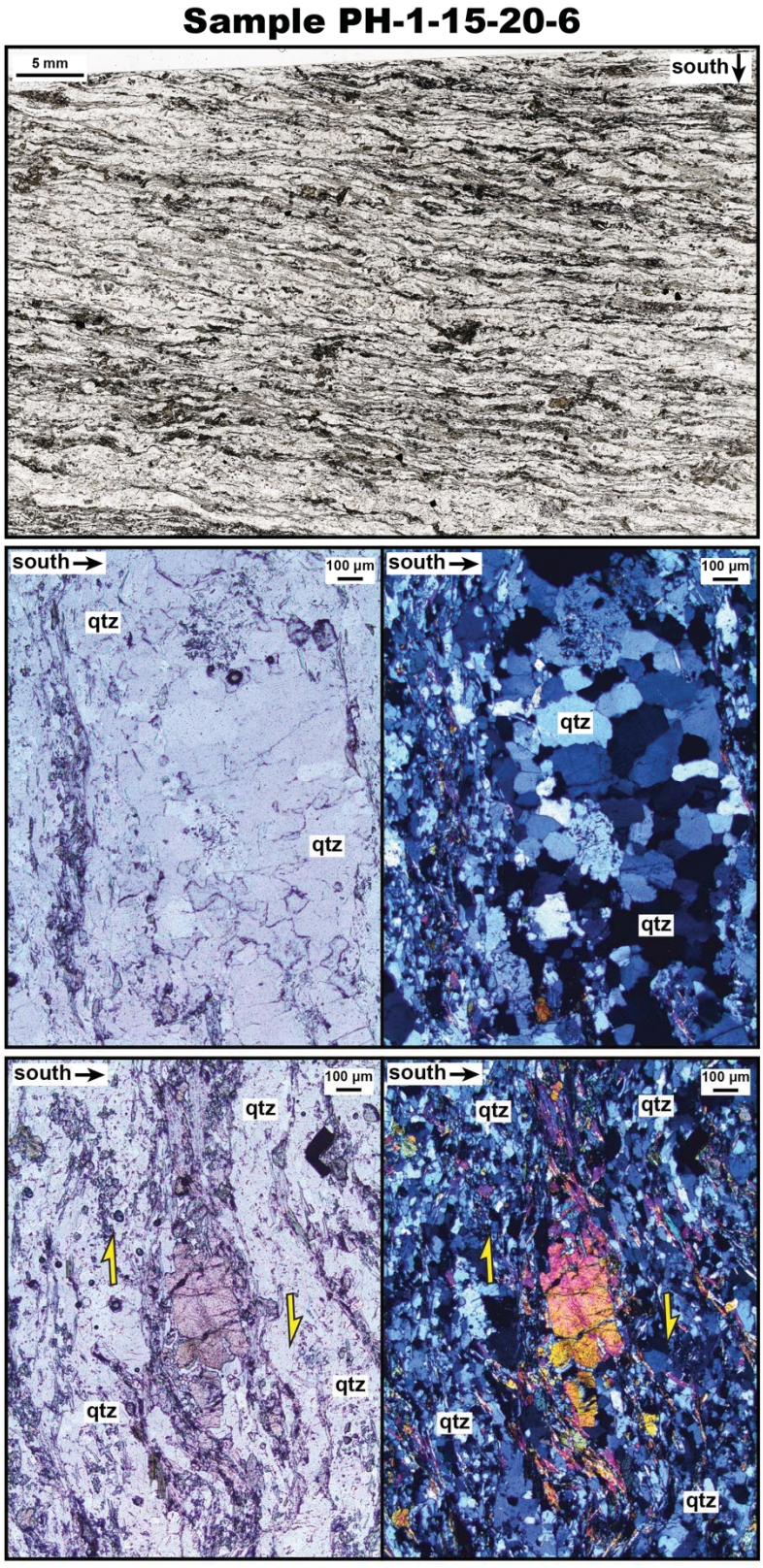

Figure S25. Plane-polarized (top and bottom left) and cross-polarized-light (bottom right) photomicrographs of EBSD sample PH-1-15-20-8.

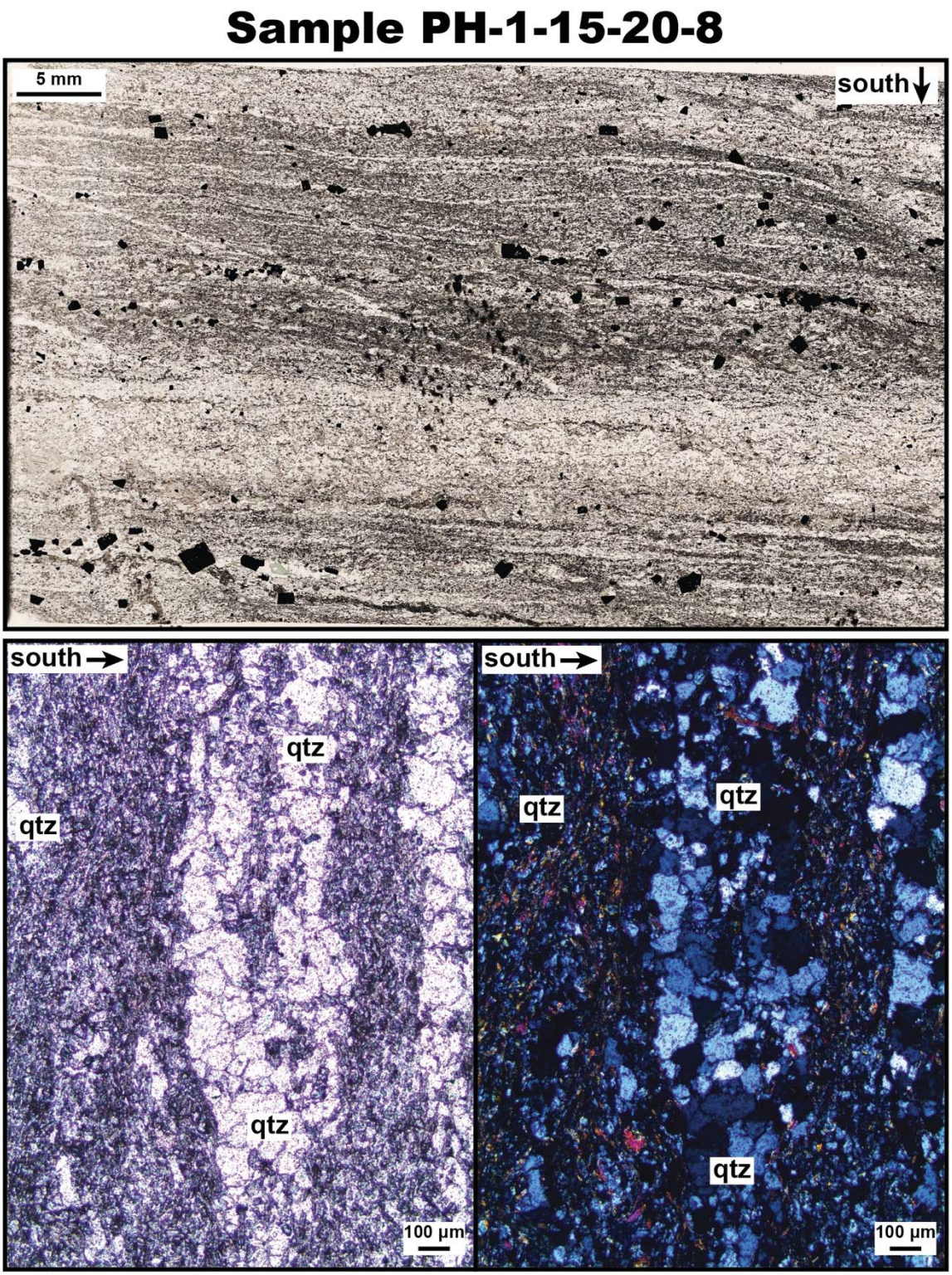

Figure S26. Plane-polarized (left) and cross-polarized-light (right) photomicrographs of EBSD sample PH-1-15-20-14.

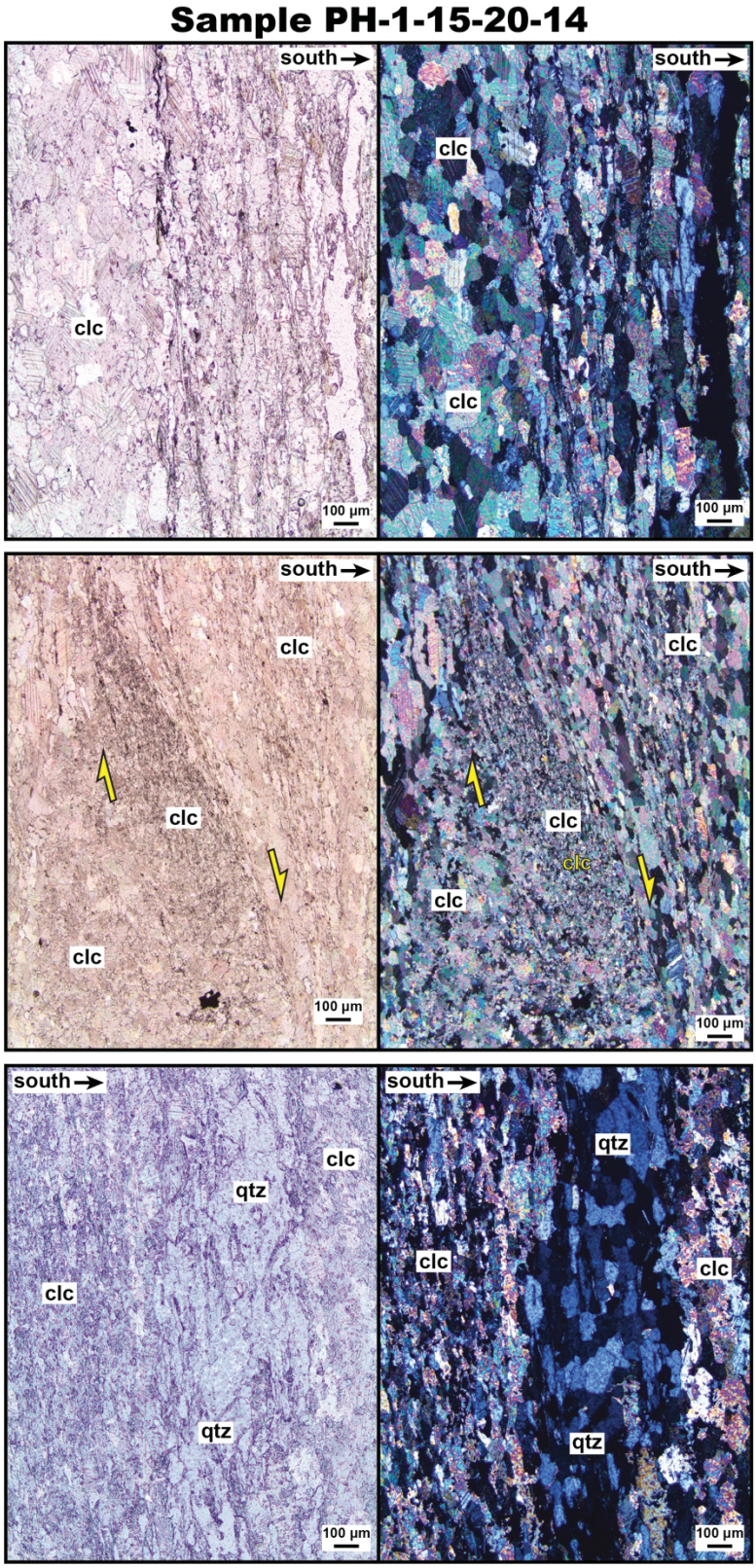

Figure S27. Plots of (A) whole-rock Sr/Y and La/Yb ratios versus U–Pb zircon crystallization age, and (B) crustal thickness versus U–Pb zircon crystallization age for Lohit Plutonic Complex samples. Crustal thicknesses and Sr/Y and La/Yb paired calibrations were determined using the method of Sundell et al. (2021). Data are compiled from this study, Lin et al. (2013), Haproff et al. (2019), and Bikramaditya et al. (2020).

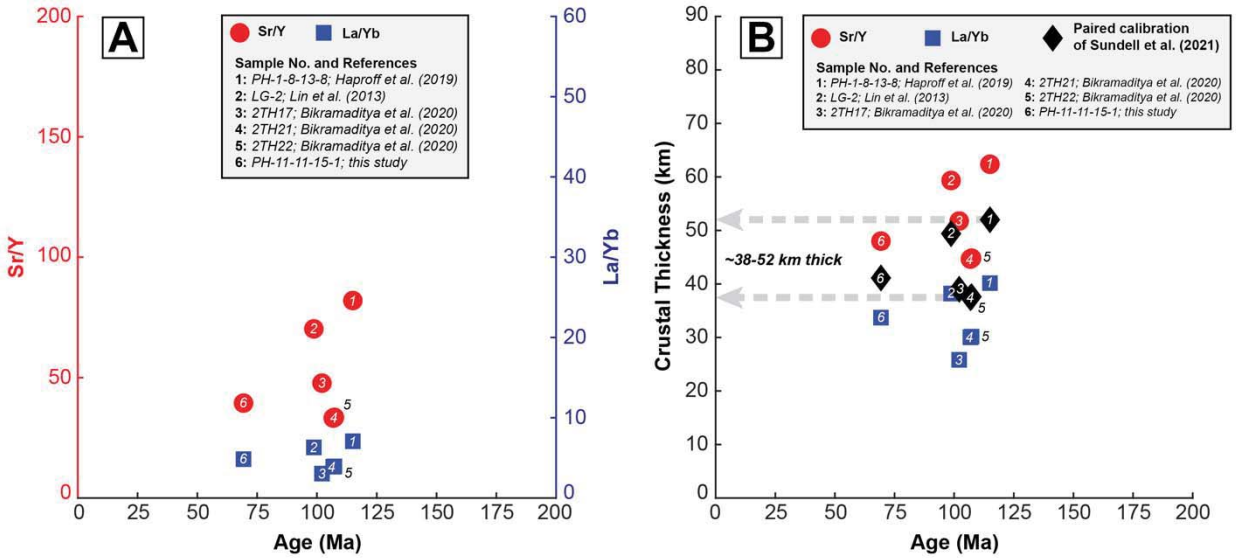

Table S1. Analytical details of zircon U–Pb geochronology.

Sample.Grain #	[U] ppm	U/Th	207/235	2σ Prop error	206/238	2σ Prop error	RHO	207/235 Age Ma	2σ Prop error	206/238 Age (Ma)	2σ Prop error	207/206 Age (Ma)	2σ Prop error	Best age (Ma)	2σ Prop error	% Discordance
PH1-11-18-4_1.FIN2	240.3	2.28	0.1083	0.0061	0.01591	0.00029	0.10	103.8	5.5	101.8	1.9	150	110	101.8	1.9	1.9
PH1-11-18-4_2.FIN2	217.3	4.37	0.1106	0.0073	0.01549	0.00034	0.16	105.8	6.6	99.1	2.2	240	130	99.1	2.2	6.3
PH1-11-18-4_3.FIN2	421	6.46	0.1087	0.0047	0.01614	0.00029	0.12	104.4	4.3	103.2	1.8	143	87	103.2	1.8	1.1
PH1-11-18-4_4.FIN2	93.4	3.80	0.113	0.011	0.01584	0.00043	0.03	110	10	101.3	2.8	200	170	101.3	2.8	7.9
PH1-11-18-4_5.FIN2	228.9	4.49	0.102	0.0068	0.01543	0.00035	0.02	98	6.2	98.7	2.2	90	120	98.7	2.2	0.7
PH1-11-18-4_6.FIN2	129.4	4.13	0.15	0.012	0.01568	0.00045	0.18	140	10	100.3	2.9	720	160	100.3	2.9	28.4
PH1-11-18-4_7.FIN2	252.2	6.10	0.1046	0.0057	0.01552	0.00029	0.06	101.2	5.3	99.2	1.9	140	110	99.2	1.9	2.0
PH1-11-18-4_8.FIN2	131.8	2.98	0.1289	0.0099	0.01539	0.00043	0.17	122.1	8.9	98.4	2.7	520	160	98.4	2.7	19.4
PH1-11-18-4_9.FIN2	208	3.75	0.1009	0.0071	0.01499	0.00041	0.03	97	6.5	95.9	2.6	150	140	95.9	2.6	1.1
PH1-11-18-4_10.FIN2	508.2	5.28	0.1045	0.0049	0.01515	0.00022	0.02	101.2	4.6	97	1.4	175	93	97.0	1.4	4.2
PH1-11-18-4_11.FIN2	218.5	4.62	0.1086	0.0061	0.01525	0.00034	0.05	104.1	5.6	97.6	2.1	230	110	97.6	2.1	6.2
PH1-11-18-4_12.FIN2	218.8	4.16	0.11	0.0071	0.01551	0.00037	0.01	105.3	6.4	99.2	2.4	210	130	99.2	2.4	5.8
PH1-11-18-4_13.FIN2	544	3.94	0.1037	0.0039	0.01582	0.00023	0.08	100	3.5	101.2	1.5	72	75	101.2	1.5	1.2
PH1-11-18-4_14.FIN2	1929	3.63	0.1072	0.0039	0.01535	0.00024	0.30	103.3	3.6	98.2	1.5	189	73	98.2	1.5	4.9
PH1-11-18-4_15.FIN2	295.5	2.63	0.2203	0.0088	0.01662	0.0003	0.14	201.2	7.2	106.2	1.9	1481	80	DISC	DISC	47.2
PH1-11-18-4_16.FIN2	419	3.94	0.1006	0.0051	0.01522	0.00025	0.14	97	4.7	97.4	1.6	122	99	97.4	1.6	0.4
PH1-11-18-4_17.FIN2	249	3.08	0.1838	0.0096	0.01589	0.00038	0.05	170.4	8.2	101.6	2.4	1200	120	DISC	DISC	40.4
PH1-11-18-4_18.FIN2	363	5.30	0.1153	0.0053	0.01515	0.00026	0.22	110.4	4.8	97	1.7	360	91	97.0	1.7	12.1
PH1-11-18-4_19.FIN2	363	6.66	0.1156	0.0059	0.01639	0.00026	0.03	110.5	5.4	104.8	1.7	220	100	104.8	1.7	5.2
PH1-11-18-4_20.FIN2	114.2	5.46	0.107	0.0094	0.01606	0.00004	0.07	101.8	8.5	102.7	2.6	70	150	102.7	2.6	0.9
PH1-11-18-4_21.FIN2	325	6.81	0.1092	0.006	0.016	0.00036	0.00	104.7	5.5	102.3	2.3	160	110	102.3	2.3	2.3
PH1-11-18-4_22.FIN2	266.1	5.50	0.1067	0.006	0.01554	0.00029	0.11	102.5	5.5	99.4	1.8	190	110	99.4	1.8	3.0
PH1-11-18-4_23.FIN2	129.1	-0.42	0.1093	0.008	0.01587	0.00042	0.10	104.3	7.3	101.5	2.6	140	130	101.5	2.6	2.7
PH1-11-18-4_24.FIN2	255	3.58	0.1041	0.0052	0.01549	0.00032	0.03	100.2	4.8	99.1	2	140	100	99.1	2.0	1.1
PH1-11-18-4_25.FIN2	174	5.50	0.0962	0.0065	0.01559	0.00035	0.05	92.6	6	99.7	2.2	-10	120	99.7	2.2	7.7
PH1-11-18-4_26.FIN2	242	8.83	0.1077	0.0059	0.01554	0.00033	0.13	103.3	5.4	99.4	2.1	180	100	99.4	2.1	3.8
PH1-11-18-4_27.FIN2	381	8.28	0.1067	0.0059	0.01591	0.00036	0.01	103.1	5.5	101.8	2.3	150	110	101.8	2.3	1.3
PH1-11-18-4_28.FIN2	240.7	5.29	0.101	0.0057	0.01537	0.00029	0.14	97.8	5.4	98.5	1.9	80	100	98.5	1.9	0.7
PH1-11-18-4_29.FIN2	325	4.17	0.1011	0.0054	0.01527	0.00025	0.10	98.6	5.2	97.7	1.6	117	99	97.7	1.6	0.9
PH1-11-18-4_30.FIN2	901	3.31	0.1111	0.0041	0.01592	0.00022	0.05	106.8	3.8	101.8	1.4	209	79	101.8	1.4	4.7
PH1-11-18-4_31.FIN2	229.8	4.10	0.1093	0.0063	0.01606	0.00033	0.05	104.7	5.7	102.7	2.1	150	110	102.7	2.1	1.9
PH1-11-18-4_32.FIN2	2482	8.39	0.1027	0.002	0.01494	0.00016	0.24	99.3	1.8	95.57	0.99	162	40	95.6	1.0	3.8
PH1-11-18-4_33.FIN2	97	9.02	0.0967	0.0081	0.01534	0.00045	0.02	92.7	7.4	98.1	2.8	70	150	98.1	2.8	5.8
PH1-11-18-4_34.FIN2	175	14.40	0.113	0.0086	0.01559	0.00041	0.08	108.6	7.9	99.7	2.6	260	150	99.7	2.6	8.2

PH1-11-18-4_35.FIN2	476	10.79	0.1039	0.0043	0.01555	0.00023	0.12	100.1	3.9	99.4	1.5	120	79	99.4	1.5	0.7
PH1-11-18-4_36.FIN2	154.8	3.67	0.161	0.012	0.01629	0.00049	0.05	152	11	104.1	3.1	860	170	DISC	DISC	31.5
PH1-11-18-4_37.FIN2	200.8	5.25	0.141	0.014	0.01637	0.00054	0.10	133	12	104.7	3.4	590	200	104.7	3.4	21.3
PH1-11-18-4_38.FIN2	245.7	5.21	0.1068	0.0055	0.01573	0.0003	0.16	102.6	5	100.6	1.9	150	99	100.6	1.9	1.9
PH1-11-18-4_39.FIN2	200.7	5.66	0.158	0.009	0.01547	0.00034	0.11	148.8	8	98.9	2.2	930	120	DISC	DISC	33.5
PH1-11-18-4_40.FIN2	250.3	4.89	0.1059	0.0055	0.01599	0.00037	0.11	101.8	5.1	102.3	2.4	100	96	102.3	2.4	0.5
PH1-11-18-4_41.FIN2	202.9	6.02	0.1091	0.0057	0.01564	0.00033	0.05	104.6	5.2	100	2.1	220	110	100.0	2.1	4.4
PH1-11-18-4_42.FIN2	282	7.92	0.1109	0.006	0.01553	0.00032	0.08	106.3	5.5	99.3	2	270	120	99.3	2.0	6.6
PH1-11-18-4_43.FIN2	127.2	6.30	0.123	0.013	0.01589	0.00062	0.09	117	12	101.6	3.9	340	210	101.6	3.9	13.2
PH1-11-18-4_44.FIN2	254.2	8.23	0.1021	0.0068	0.01568	0.00029	0.10	98	6.2	100.3	1.8	60	120	100.3	1.8	2.3
PH1-11-18-4_45.FIN2	217	8.46	0.1029	0.0062	0.01565	0.00036	0.05	98.8	5.7	100.1	2.3	90	110	100.1	2.3	1.3
PH1-11-18-4_46.FIN2	167.9	10.50	0.1086	0.0074	0.01535	0.00039	0.01	103.9	6.7	98.2	2.4	210	130	98.2	2.4	5.5
PH1-11-18-4_47.FIN2	223.4	8.54	0.0986	0.0062	0.01516	0.00028	0.06	94.9	5.7	97	1.8	100	120	97.0	1.8	2.2
PH1-11-18-4_48.FIN2	232.5	5.01	0.1042	0.006	0.01545	0.00032	0.07	100.1	5.5	98.8	2	130	110	98.8	2.0	1.3
PH1-11-18-4_49.FIN2	355	4.87	0.1302	0.0063	0.0154	0.00029	0.10	123.7	5.6	98.5	1.8	600	110	98.5	1.8	20.4
PH1-11-18-4_50.FIN2	268	6.31	0.1219	0.006	0.01563	0.0003	0.05	116.2	5.4	100	1.9	420	100	100.0	1.9	13.9
PH1-11-18-4_51.FIN2	264.8	6.43	0.1134	0.0056	0.01589	0.00029	0.01	108.6	5.1	101.6	1.8	280	100	101.6	1.8	6.4
PH1-11-18-4_52.FIN2	321	7.15	0.1051	0.0046	0.01593	0.0003	0.06	101.2	4.3	101.9	1.9	105	88	101.9	1.9	0.7
PH1-11-18-4_53.FIN2	161	6.51	0.1156	0.0093	0.01581	0.00041	0.05	110	8.3	101.1	2.6	250	150	101.1	2.6	8.1
PH1-11-18-4_54.FIN2	237.8	4.84	0.1067	0.0065	0.01508	0.0003	0.19	103	6.1	96.4	1.9	220	110	96.4	1.9	6.4
PH1-11-18-4_55.FIN2	273.4	5.68	0.1062	0.0056	0.0154	0.00032	0.21	102	5.1	98.5	2	200	100	98.5	2.0	3.4
PH1-11-18-4_56.FIN2	39.2	-4.00	0.153	0.018	0.01572	0.00074	0.10	142	16	100.5	4.7	640	230	100.5	4.7	29.2
PH1-11-18-4_58.FIN2	358	3.26	0.1194	0.0057	0.01631	0.00029	0.03	114	5.2	104.3	1.9	300	100	104.3	1.9	8.5
PH1-11-18-4_59.FIN2	226.1	6.59	0.1009	0.0058	0.01584	0.00033	0.31	97.1	5.4	101.3	2.1	60	100	101.3	2.1	4.3
PH1-11-18-4_60.FIN2	300.2	5.22	0.1035	0.0049	0.01538	0.00028	0.21	99.6	4.5	98.4	1.8	143	92	98.4	1.8	1.2
PH1-11-18-4_61.FIN2	124.8	13.80	0.1415	0.0097	0.0153	0.00046	0.08	133	8.5	97.9	2.9	730	150	97.9	2.9	26.4
PH1-11-18-4_62.FIN2	344	4.26	0.1049	0.0057	0.01556	0.00031	0.15	100.8	5.2	99.6	1.9	130	100	99.6	1.9	1.2
PH1-11-18-4_63.FIN2	287.7	6.07	0.1005	0.0054	0.01513	0.00029	0.00	96.8	5	96.8	1.9	120	100	96.8	1.9	0.0
PH1-11-18-4_64.FIN2	232.4	7.27	0.0993	0.006	0.01544	0.00032	0.09	96.3	5.7	98.7	2	70	110	98.7	2.0	2.5
PH1-11-18-4_65.FIN2	242.6	7.11	0.1081	0.0062	0.01532	0.00037	0.13	103.6	5.7	98	2.3	230	110	98.0	2.3	5.4
PH1-11-18-4_66.FIN2	168.2	5.74	0.1101	0.0081	0.01561	0.00037	0.09	106	7.6	99.8	2.3	230	140	99.8	2.3	5.8
PH1-11-18-4_67.FIN2	369.8	3.46	0.1017	0.0053	0.01522	0.00029	0.11	98	4.9	97.4	1.9	140	110	97.4	1.9	0.6
PH1-11-18-4_68.FIN2	254	7.80	0.1164	0.0063	0.01602	0.00038	0.15	111.2	5.7	102.5	2.4	290	110	102.5	2.4	7.8
PH1-11-18-4_69.FIN2	316	4.69	0.1038	0.0053	0.01604	0.0003	0.07	99.8	4.9	102.6	1.9	66	96	102.6	1.9	2.8
PH1-11-18-4_70.FIN2	276.8	4.21	0.1149	0.0059	0.01522	0.00027	0.06	109.9	5.4	97.4	1.7	350	100	97.4	1.7	11.4
PH1-11-18-4_71.FIN2	221	10.21	0.1048	0.007	0.01589	0.00035	0.03	100.4	6.4	101.6	2.2	70	120	101.6	2.2	1.2
PH1-11-18-4_72.FIN2	104	6.40	0.126	0.011	0.0161	0.00055	0.01	118.3	10	102.9	3.5	360	170	102.9	3.5	13.0
PH1-11-18-4_73.FIN2	54.8	5.20	0.106	0.012	0.0151	0.0006	0.25	100	11	96.5	3.8	80	200	96.5	3.8	3.5

PH1-11-18-4_74.FIN2	193	5.85	0.1123	0.0076	0.01596	0.00037	0.01	107.2	6.8	102	2.4	190	120	102.0	2.4	4.9
PH1-11-18-4_75.FIN2	135.3	3.87	0.238	0.025	0.01791	0.00009	0.26	215	20	114.4	5.7	1520	220	DISC	DISC	46.8
PH1-11-18-4_76.FIN2	433	3.20	0.1172	0.009	0.01605	0.00042	0.15	112.1	8.1	102.6	2.7	260	150	102.6	2.7	8.5
PH1-11-18-4_77.FIN2	245.5	5.60	0.0984	0.0054	0.01537	0.00031	0.03	94.8	5	98.3	2	60	100	98.3	2.0	3.7
PH1-11-18-4_78.FIN2	267	5.23	0.1208	0.0061	0.01577	0.00003	0.00	115.2	5.5	100.8	1.9	390	110	100.8	1.9	12.5
PH1-11-18-4_79.FIN2	307	3.48	0.1297	0.0076	0.01492	0.00039	0.06	123.3	6.8	95.5	2.5	640	130	95.5	2.5	22.5
PH1-11-18-4_80.FIN2	171	6.50	0.152	0.017	0.01656	0.00076	0.27	143	15	105.9	4.8	670	220	105.9	4.8	25.9
PH1-11-18-4_81.FIN2	268	13.60	0.107	0.015	0.01583	0.00059	0.12	102	14	101.2	3.8	110	240	101.2	3.8	0.8
PH1-11-18-4_82.FIN2	1504	3.96	0.0958	0.0041	0.01354	0.00024	0.02	92.8	3.8	86.7	1.5	165	92	86.7	1.5	6.6
PH1-11-18-4_83.FIN2	296.5	3.51	0.1059	0.0052	0.01531	0.00028	0.24	102.4	4.9	97.9	1.8	207	94	97.9	1.8	4.4
PH1-11-18-4_84.FIN2	149	-13.00	0.127	0.012	0.01568	0.00068	0.01	121	11	100.3	4.3	510	220	100.3	4.3	17.1
PH1-11-18-4_85.FIN2	236.7	5.86	0.1051	0.0063	0.01567	0.00032	0.06	100.8	5.8	100.2	2	140	110	100.2	2.0	0.6
PH1-11-18-4_86.FIN2	170.8	5.07	0.1261	0.0076	0.01534	0.00032	0.01	120.6	7	98.1	2	500	120	98.1	2.0	18.7
PH1-11-18-4_87.FIN2	429.8	3.23	0.1387	0.0086	0.01529	0.00041	0.02	131.4	7.6	97.8	2.6	740	140	97.8	2.6	25.6
PH1-11-18-4_88.FIN2	153.9	5.86	0.1395	0.0085	0.01561	0.00037	0.10	132.4	7.7	99.8	2.3	650	130	99.8	2.3	24.6
PH1-11-18-4_89.FIN2	194.3	3.51	0.1038	0.0067	0.01573	0.00038	0.06	99.5	6.1	100.6	2.4	100	120	100.6	2.4	1.1
PH1-11-18-4_90.FIN2	260.4	4.75	0.1162	0.0068	0.01549	0.00031	0.11	111.7	6.3	99.1	2	340	110	99.1	2.0	11.3
PH1-11-18-4_91.FIN2	566	2.40	0.1043	0.0042	0.01492	0.00026	0.22	100.9	4	95.4	1.6	211	79	95.4	1.6	5.5
PH1-11-18-4_92.FIN2	265	5.73	0.158	0.0089	0.01621	0.00037	0.10	148	7.8	103.6	2.4	860	120	DISC	DISC	30.0
PH1-11-18-4_93.FIN2	130.8	3.74	0.143	0.011	0.01614	0.00045	0.02	134.1	9.6	103.2	2.9	610	150	103.2	2.9	23.0
PH1-11-18-4_94.FIN2	175.6	5.41	0.101	0.0072	0.0156	0.00039	0.06	96.9	6.6	99.8	2.5	50	130	99.8	2.5	3.0
PH1-11-18-4_95.FIN2	197	2.25	0.1097	0.0085	0.01639	0.00004	0.19	104.8	7.7	104.8	2.5	120	140	104.8	2.5	0.0
PH1-11-18-4_96.FIN2	260	5.50	0.107	0.0063	0.01561	0.00032	0.08	102.6	5.8	99.8	2	160	110	99.8	2.0	2.7
PH1-11-18-4_97.FIN2	461	2.83	0.1101	0.0049	0.01597	0.00029	0.23	106.9	4.7	102.1	1.9	199	86	102.1	1.9	4.5
PH1-11-18-4_98.FIN2	212.5	5.18	0.162	0.0086	0.01604	0.00031	0.09	153.3	7.9	102.6	2	940	120	DISC	DISC	33.1
PH1-11-18-4_99.FIN2	218.6	4.07	0.172	0.012	0.0162	0.00045	0.06	161	10	103.6	2.8	1060	160	DISC	DISC	35.7
PH1-11-18-4_100.FIN2	234.6	4.26	0.1101	0.0075	0.01534	0.00035	0.02	105.4	6.9	98.1	2.2	240	130	98.1	2.2	6.9
PH1-11-18-4_101.FIN2	100.6	5.90	0.131	0.01	0.0161	0.00043	0.13	123.2	9.4	102.9	2.7	420	150	102.9	2.7	16.5
PH1-11-18-4_102.FIN2	372	3.50	0.106	0.0057	0.01512	0.00032	0.19	101.9	5.2	96.7	2	220	100	96.7	2.0	5.1
PH1-11-18-4_103.FIN2	269	3.31	0.1038	0.0058	0.01508	0.00003	0.12	99.7	5.3	96.5	1.9	170	110	96.5	1.9	3.2
PH1-11-18-4_104.FIN2	287	5.32	0.1383	0.0075	0.01515	0.00029	0.13	130.9	6.6	97	1.8	720	120	97.0	1.8	25.9
PH1-11-18-4_105.FIN2	131.7	2.68	0.14	0.015	0.01804	0.00059	0.20	131	14	115.3	3.8	370	230	115.3	3.8	12.0
PH1-11-18-4_106.FIN2	826	3.33	0.0997	0.0034	0.0148	0.00023	0.27	96.3	3.1	94.7	1.5	148	67	94.7	1.5	1.7
PH1-11-18-4_107.FIN2	220	6.53	0.1097	0.0066	0.01619	0.00033	0.16	105.1	5.9	103.5	2.1	140	110	103.5	2.1	1.5
PH1-11-18-4_108.FIN2	253	4.66	0.1099	0.0083	0.01519	0.00039	0.14	105.4	7.5	97.2	2.5	260	150	97.2	2.5	7.8
PH1-11-18-4_109.FIN2	151	18.20	0.145	0.014	0.01665	0.00073	0.20	136	13	106.4	4.6	630	210	106.4	4.6	21.8
PH1-11-18-4_110.FIN2	245	2.56	0.148	0.012	0.01568	0.00052	0.40	139	11	100.3	3.3	830	160	100.3	3.3	27.8

PH1-14-20-9_1.FIN2	186.2	8.63	0.0896	0.0057	0.01303	0.00031	0.06	86.6	5.3	83.4	2	180	120	83.4	2.0	3.7
PH1-14-20-9_2.FIN2	153.1	7.32	0.0842	0.0063	0.01296	0.00031	0.13	81.4	5.8	83	2	50	130	83.0	2.0	2.0
PH1-14-20-9_3.FIN2	274	10.18	0.0719	0.0048	0.0118	0.00027	0.10	70.7	4.7	75.6	1.7	-20	120	75.6	1.7	6.9
PH1-14-20-9_4.FIN2	384	14.00	0.085	0.0043	0.01313	0.00027	0.00	82.6	4.1	84.1	1.7	80	100	84.1	1.7	1.8
PH1-14-20-9_5.FIN2	1002	28.10	0.0872	0.0027	0.01283	0.00017	0.07	84.7	2.5	82.2	1.1	167	63	82.2	1.1	3.0
PH1-14-20-9_6.FIN2	323.7	10.22	0.085	0.0044	0.01284	0.00022	0.06	82.5	4.1	82.2	1.4	101	98	82.2	1.4	0.4
PH1-14-20-9_7.FIN2	536	25.90	0.0896	0.0037	0.01366	0.00024	0.10	86.9	3.4	87.4	1.5	94	80	87.4	1.5	0.6
PH1-14-20-9_8.FIN2	165.2	8.62	0.0797	0.0061	0.01292	0.00031	0.08	77.2	5.7	82.8	2	-20	130	82.8	2.0	7.3
PH1-14-20-9_9.FIN2	563	18.39	0.0823	0.0033	0.01238	0.0002	0.13	80.1	3.1	79.3	1.2	120	80	79.3	1.2	1.0
PH1-14-20-9_10.FIN2	249.5	6.01	0.0834	0.0051	0.01261	0.00027	0.11	80.9	4.7	80.8	1.7	110	110	80.8	1.7	0.1
PH1-14-20-9_11.FIN2	203.4	12.04	0.083	0.0048	0.013	0.00032	0.01	80.6	4.4	83.3	2	70	110	83.3	2.0	3.3
PH1-14-20-9_12.FIN2	504	8.66	0.0819	0.0037	0.01216	0.00021	0.05	79.7	3.5	77.9	1.4	139	90	77.9	1.4	2.3
PH1-14-20-9_13.FIN2	1179	7.71	0.081	0.0025	0.01219	0.00014	0.18	79	2.3	78.08	0.89	114	60	78.1	0.9	1.2
PH1-14-20-9_14.FIN2	403	18.30	0.0881	0.0043	0.01305	0.00026	0.09	85.9	4.1	83.6	1.6	147	95	83.6	1.6	2.7
PH1-14-20-9_15.FIN2	284	12.58	0.0907	0.005	0.01307	0.00026	0.00	87.7	4.6	83.7	1.6	200	110	83.7	1.6	4.6
PH1-14-20-9_16.FIN2	259.6	8.08	0.0822	0.0049	0.01312	0.00028	0.13	79.8	4.6	84	1.8	0	110	84.0	1.8	5.3
PH1-14-20-9_17.FIN2	1221	33.50	0.083	0.0025	0.01255	0.00014	0.17	80.8	2.3	80.4	0.89	108	59	80.4	0.9	0.5
PH1-14-20-9_18.FIN2	251.8	12.92	0.0862	0.0048	0.01302	0.00027	0.05	84.2	4.5	83.4	1.7	120	110	83.4	1.7	1.0
PH1-14-20-9_19.FIN2	144.4	9.66	0.0876	0.0062	0.01279	0.00036	0.16	84.6	5.8	81.9	2.3	180	140	81.9	2.3	3.2
PH1-14-20-9_20.FIN2	184.6	20.70	0.0839	0.0059	0.01229	0.00031	0.24	81.3	5.5	78.7	2	160	130	78.7	2.0	3.2
PH1-14-20-9_21.FIN2	336	9.36	0.0806	0.0043	0.01224	0.00023	0.01	78.4	4	78.4	1.4	100	100	78.4	1.4	0.0
PH1-14-20-9_22.FIN2	220	12.33	0.087	0.0054	0.01245	0.00028	0.00	84.2	5	79.7	1.8	230	120	79.7	1.8	5.3
PH1-14-20-9_23.FIN2	431	8.73	0.0873	0.0043	0.01327	0.00024	0.07	85.2	4.1	85	1.5	98	93	85.0	1.5	0.2
PH1-14-20-9_24.FIN2	193.9	7.37	0.0872	0.0058	0.01265	0.00029	0.04	85	5.5	81	1.8	180	120	81.0	1.8	4.7
PH1-14-20-9_25.FIN2	279.6	8.43	0.0823	0.0047	0.0129	0.00025	0.06	79.9	4.4	82.6	1.6	40	100	82.6	1.6	3.4
PH1-14-20-9_26.FIN2	1018	30.01	0.0896	0.003	0.01313	0.00018	0.18	87	2.8	84.1	1.1	154	68	84.1	1.1	3.3
PH1-14-20-9_27.FIN2	268.1	5.45	0.0823	0.005	0.01255	0.00021	0.01	79.9	4.6	80.4	1.4	90	110	80.4	1.4	0.6
PH1-14-20-9_28.FIN2	625	13.41	0.0805	0.0032	0.01208	0.00017	0.14	78.4	3	77.4	1.1	125	77	77.4	1.1	1.3
PH1-14-20-9_29.FIN2	202.9	13.40	0.0859	0.0079	0.01317	0.00041	0.22	83.2	7.4	84.3	2.6	110	180	84.3	2.6	1.3
PH1-14-20-9_30.FIN2	219.6	9.98	0.086	0.0058	0.01264	0.00028	0.03	83.2	5.4	81	1.8	140	120	81.0	1.8	2.6
PH1-14-20-9_31.FIN2	1293	36.00	0.0862	0.0025	0.01317	0.00019	0.15	83.8	2.4	84.3	1.2	96	61	84.3	1.2	0.6
PH1-14-20-9_32.FIN2	152	7.63	0.0825	0.0063	0.01288	0.00032	0.15	80.5	6	82.5	2.1	60	140	82.5	2.1	2.5
PH1-14-20-9_33.FIN2	212.8	9.77	0.0876	0.0059	0.01283	0.00027	0.07	84.7	5.4	82.2	1.7	140	120	82.2	1.7	3.0
PH1-14-20-9_34.FIN2	232	-9.00	0.0803	0.0055	0.01153	0.00025	0.08	77.9	5.2	73.9	1.6	180	130	73.9	1.6	5.1
PH1-14-20-9_35.FIN2	99.4	13.10	0.082	0.0078	0.01245	0.00042	0.03	79	7.2	79.7	2.7	60	170	79.7	2.7	0.9
PH1-14-20-9_36.FIN2	1020	29.40	0.0884	0.0034	0.01292	0.00024	0.07	85.9	3.1	82.8	1.5	169	74	82.8	1.5	3.6
PH1-14-20-9_37.FIN2	183.9	11.66	0.082	0.0059	0.01251	0.00031	0.11	79.4	5.5	80.2	2	100	130	80.2	2.0	1.0
PH1-14-20-9_38.FIN2	251.4	13.01	0.082	0.0051	0.01265	0.00024	0.04	79.6	4.8	81	1.5	60	110	81.0	1.5	1.8

PH1-14-20-9_39.FIN2	1400	46.10	0.0891	0.0029	0.01383	0.00023	0.22	86.5	2.7	88.5	1.5	61	62	88.5	1.5	2.3
PH1-14-20-9_40.FIN2	231.2	10.03	0.0841	0.005	0.01281	0.00028	0.10	82.2	4.8	82	1.8	100	110	82.0	1.8	0.2
PH1-14-20-9_41.FIN2	825	26.27	0.0845	0.0033	0.01309	0.00021	0.20	82.2	3.1	83.8	1.4	64	73	83.8	1.4	1.9
PH1-14-20-9_42.FIN2	323.1	12.94	0.0819	0.0037	0.01281	0.00024	0.00	79.7	3.5	82.1	1.5	69	93	82.1	1.5	3.0
PH1-14-20-9_43.FIN2	346.8	20.50	0.0831	0.0043	0.01261	0.00023	0.14	80.7	4	80.8	1.5	113	98	80.8	1.5	0.1
PH1-14-20-9_44.FIN2	1470	43.10	0.0836	0.0028	0.01259	0.00017	0.28	81.4	2.6	80.6	1.1	108	63	80.6	1.1	1.0
PH1-14-20-9_45.FIN2	227.6	10.74	0.0843	0.0056	0.01257	0.00026	0.05	81.7	5.2	80.5	1.6	120	120	80.5	1.6	1.5
PH1-14-20-9_46.FIN2	210.6	12.42	0.0864	0.0054	0.01283	0.0003	0.05	84.3	5.1	82.2	1.9	150	120	82.2	1.9	2.5
PH1-14-20-9_47.FIN2	209.6	9.73	0.0829	0.0051	0.01289	0.00029	0.08	80.4	4.8	82.5	1.9	60	110	82.5	1.9	2.6
PH1-14-20-9_48.FIN2	403	9.08	0.0858	0.0044	0.01332	0.00027	0.01	83.3	4.1	85.3	1.7	67	100	85.3	1.7	2.4
PH1-14-20-9_49.FIN2	213.3	10.11	0.0814	0.0055	0.01273	0.00029	0.12	79	5.2	81.5	1.8	30	120	81.5	1.8	3.2
PH1-14-20-9_50.FIN2	536	17.57	0.0839	0.0033	0.01235	0.00022	0.11	81.7	3.1	79.1	1.4	164	80	79.1	1.4	3.2
PH1-14-20-9_51.FIN2	229.3	11.48	0.0834	0.0053	0.01254	0.00026	0.04	81.5	5.1	80.4	1.7	120	120	80.4	1.7	1.3
PH1-14-20-9_52.FIN2	222.9	11.25	0.0777	0.0049	0.01253	0.00031	0.02	75.5	4.6	80.2	2	0	110	80.2	2.0	6.2
PH1-14-20-9_53.FIN2	225.6	10.42	0.0802	0.0047	0.01265	0.0003	0.13	78	4.4	81	1.9	40	110	81.0	1.9	3.8
PH1-14-20-9_54.FIN2	228.1	12.80	0.0868	0.0049	0.01243	0.00024	0.04	84.1	4.5	79.6	1.5	200	110	79.6	1.5	5.4
PH1-14-20-9_55.FIN2	394	20.07	0.0883	0.0045	0.0131	0.00025	0.12	86.1	4.2	83.9	1.6	144	96	83.9	1.6	2.6
PH1-14-20-9_56.FIN2	191.1	8.18	0.0897	0.0062	0.01236	0.00032	0.06	86.7	5.7	79.2	2.1	270	130	79.2	2.1	8.7
PH1-14-20-9_57.FIN2	278.1	11.65	0.0832	0.0046	0.01283	0.00026	0.01	80.8	4.3	82.2	1.6	80	100	82.2	1.6	1.7
PH1-14-20-9_58.FIN2	217.2	10.60	0.0809	0.0056	0.01256	0.00029	0.07	78.5	5.2	80.5	1.9	40	120	80.5	1.9	2.5
PH1-14-20-9_59.FIN2	243.7	11.51	0.0766	0.0048	0.01254	0.00029	0.05	74.6	4.5	80.3	1.8	-30	110	80.3	1.8	7.6
PH1-14-20-9_60.FIN2	361	16.50	0.0857	0.005	0.01277	0.00025	0.17	83.1	4.7	81.8	1.6	110	100	81.8	1.6	1.6
PH1-14-20-9_61.FIN2	217.3	13.25	0.081	0.0049	0.01251	0.00028	0.13	79.2	4.7	80.1	1.8	80	110	80.1	1.8	1.1
PH1-14-20-9_62.FIN2	381.9	14.53	0.0906	0.0044	0.01243	0.00023	0.00	87.7	4.1	79.6	1.5	300	100	79.6	1.5	9.2
PH1-14-20-9_63.FIN2	203.5	10.75	0.0852	0.0053	0.01269	0.0003	0.12	82.6	4.9	81.3	1.9	140	120	81.3	1.9	1.6
PH1-14-20-9_64.FIN2	145.9	13.14	0.0792	0.0062	0.01251	0.00033	0.01	77.6	6	80.1	2.1	30	140	80.1	2.1	3.2
PH1-14-20-9_65.FIN2	254.6	13.61	0.083	0.0056	0.01282	0.00026	0.20	80.5	5.2	82.1	1.7	40	120	82.1	1.7	2.0
PH1-14-20-9_66.FIN2	198.9	9.95	0.0836	0.0058	0.01292	0.00029	0.00	80.9	5.4	82.8	1.8	50	120	82.8	1.8	2.3
PH1-14-20-9_67.FIN2	1168	32.10	0.0873	0.0028	0.01329	0.00018	0.03	84.8	2.6	85.1	1.2	98	64	85.1	1.2	0.4
PH1-14-20-9_68.FIN2	130.8	17.00	0.0839	0.0072	0.01202	0.00038	0.12	81	6.7	77	2.4	170	150	77.0	2.4	4.9
PH1-14-20-9_70.FIN2	285.7	11.49	0.082	0.0047	0.01299	0.00027	0.12	79.6	4.4	83.2	1.7	20	110	83.2	1.7	4.5
PH1-14-20-9_71.FIN2	264.7	12.05	0.0837	0.0052	0.0128	0.00026	0.00	81.2	4.9	82	1.7	80	110	82.0	1.7	1.0
PH1-14-20-9_72.FIN2	372	17.30	0.095	0.0048	0.01364	0.00027	0.20	91.8	4.4	87.3	1.7	194	95	87.3	1.7	4.9
PH1-14-20-9_73.FIN2	201.9	8.29	0.0867	0.0066	0.01313	0.00029	0.01	83.8	6.1	84.1	1.9	100	140	84.1	1.9	0.4
PH1-14-20-9_74.FIN2	228.9	15.10	0.0815	0.0055	0.0128	0.00029	0.01	79.1	5.1	82	1.9	40	120	82.0	1.9	3.7
PH1-14-20-9_75.FIN2	202.1	9.71	0.0871	0.0053	0.01267	0.0003	0.03	84.4	5	81.1	1.9	170	120	81.1	1.9	3.9
PH1-14-20-9_76.FIN2	419.6	15.54	0.0908	0.0056	0.01237	0.00029	0.03	88	5.2	79.2	1.9	310	130	79.2	1.9	10.0
PH1-14-20-9_77.FIN2	242	10.34	0.0811	0.005	0.0127	0.00027	0.01	79.3	4.8	81.3	1.7	40	110	81.3	1.7	2.5
PH1-14-20-9_78.FIN2	165.8	14.70	0.086	0.0064	0.01271	0.00032	0.11	83.1	5.9	81.4	2	110	130	81.4	2.0	2.0

PH1-14-20-9_79.FIN2	150.8	17.60	0.0804	0.0067	0.01294	0.00038	0.01	77.8	6.2	82.9	2.4	-40	140	82.9	2.4	6.6
PH1-14-20-9_80.FIN2	270.3	12.39	0.0888	0.0057	0.01278	0.00026	0.10	85.8	5.3	81.9	1.6	150	120	81.9	1.6	4.5
PH1-14-20-9_81.FIN2	215.5	10.57	0.0866	0.0067	0.01285	0.00029	0.11	83.6	6.2	82.3	1.8	110	140	82.3	1.8	1.6
PH1-14-20-9_82.FIN2	271.3	12.23	0.0869	0.0051	0.01268	0.00024	0.03	84.1	4.8	81.2	1.5	140	110	81.2	1.5	3.4
PH1-14-20-9_83.FIN2	241	9.17	0.0869	0.005	0.01292	0.00029	0.11	84.2	4.6	82.7	1.9	120	110	82.7	1.9	1.8
PH1-14-20-9_84.FIN2	1141	8.44	0.0801	0.003	0.0121	0.00017	0.28	78.1	2.8	77.5	1.1	92	68	77.5	1.1	0.8
PH1-14-20-9_85.FIN2	254.2	9.50	0.0888	0.0055	0.01271	0.00027	0.02	85.9	5.1	81.4	1.7	200	120	81.4	1.7	5.2
PH1-14-20-9_86.FIN2	346	14.62	0.0812	0.004	0.01225	0.00026	0.11	79.1	3.7	78.5	1.6	102	94	78.5	1.6	0.8
PH1-14-20-9_87.FIN2	802	8.68	0.0891	0.0032	0.01314	0.00021	0.16	86.5	3	84.2	1.3	143	71	84.2	1.3	2.7
PH1-14-20-9_88.FIN2	184.1	16.60	0.0874	0.0063	0.01308	0.00003	0.06	84.4	5.9	83.8	1.9	90	130	83.8	1.9	0.7
PH1-14-20-9_89.FIN2	220.2	15.96	0.0854	0.0055	0.01286	0.00028	0.04	83.5	5.2	82.4	1.8	140	120	82.4	1.8	1.3
PH1-14-20-9_90.FIN2	331	15.50	0.0865	0.0049	0.01289	0.00026	0.24	83.8	4.6	82.5	1.7	100	100	82.5	1.7	1.6
PH1-14-20-9_91.FIN2	1174	42.70	0.0882	0.0028	0.01313	0.00019	0.24	85.7	2.6	84.1	1.2	122	62	84.1	1.2	1.9
PH1-14-20-9_92.FIN2	229.8	11.37	0.0802	0.0054	0.01279	0.00027	0.05	77.9	5.1	81.9	1.7	10	120	81.9	1.7	5.1
PH1-14-20-9_93.FIN2	395.1	10.43	0.0881	0.0041	0.01256	0.00023	0.02	85.4	3.8	80.4	1.4	197	94	80.4	1.4	5.9
PH1-14-20-9_94.FIN2	278.7	8.11	0.0827	0.005	0.0127	0.00025	0.14	80.9	4.8	81.4	1.6	50	110	81.4	1.6	0.6
PH1-14-20-9_95.FIN2	1410	21.36	0.0895	0.0028	0.01383	0.00023	0.13	87.3	2.6	88.6	1.4	58	61	88.6	1.4	1.5
PH1-14-20-9_96.FIN2	196	10.11	0.0957	0.007	0.01252	0.00035	0.05	92.3	6.5	80.2	2.2	360	150	80.2	2.2	13.1
PH1-14-20-9_97.FIN2	516	25.50	0.0871	0.0043	0.01304	0.00025	0.15	84.5	4	83.5	1.6	111	95	83.5	1.6	1.2
PH1-14-20-9_98.FIN2	512	10.16	0.0715	0.003	0.01112	0.00018	0.17	70.4	3	71.3	1.2	40	83	71.3	1.2	1.3
PH1-14-20-9_99.FIN2	226.4	9.44	0.0845	0.0059	0.01249	0.0003	0.13	81.8	5.4	80	1.9	100	120	80.0	1.9	2.2
PH11-11-15-14_1.FIN2	497	5.86	0.1138	0.0049	0.0156	0.00024	0.22	109.2	4.5	99.8	1.5	296	87	99.8	1.5	8.6
PH11-11-15-14_2.FIN2	840	4.90	0.1118	0.0036	0.01564	0.0002	0.21	107.4	3.3	100	1.3	259	67	100.0	1.3	6.9
PH11-11-15-14_3.FIN2	348	13.81	0.252	0.014	0.01731	0.00036	0.26	227	11	110.6	2.3	1681	98	DISC	DISC	51.3
PH11-11-15-14_4.FIN2	309	2.65	0.1317	0.0098	0.01795	0.00042	0.35	125.1	8.8	114.7	2.7	330	150	114.7	2.7	8.3
PH11-11-15-14_5.FIN2	420	8.37	0.1165	0.0055	0.01545	0.00033	0.26	111.5	5	98.8	2.1	380	97	98.8	2.1	11.4
PH11-11-15-14_6.FIN2	2030	3.46	0.109	0.0028	0.01505	0.00025	0.19	104.9	2.6	96.3	1.6	290	59	96.3	1.6	8.2
PH11-11-15-14_7.FIN2	155	2.70	0.136	0.0096	0.0159	0.00046	0.02	129.5	8.8	101.7	2.9	570	150	101.7	2.9	21.5
PH11-11-15-14_8.FIN2	327.1	2.55	0.1351	0.0092	0.01551	0.00041	0.07	128.2	8.2	99.2	2.6	640	160	99.2	2.6	22.6
PH11-11-15-14_9.FIN2	788	3.58	0.1446	0.0054	0.01606	0.00025	0.19	136.9	4.8	102.7	1.6	759	84	102.7	1.6	25.0
PH11-11-15-14_10.FIN2	1828	3.27	0.1047	0.0027	0.01555	0.00019	0.19	101	2.5	99.5	1.2	134	51	99.5	1.2	1.5
PH11-11-15-14_11.FIN2	163	4.66	0.124	0.011	0.01549	0.00059	0.12	120	10	99.1	3.7	460	180	99.1	3.7	17.4
PH11-11-15-14_12.FIN2	338	2.81	0.1049	0.0054	0.01584	0.00032	0.15	100.9	4.9	101.3	2	99	97	101.3	2.0	0.4
PH11-11-15-14_13.FIN2	214.8	3.69	0.1286	0.0075	0.0156	0.00035	0.08	122	6.7	99.8	2.2	510	120	99.8	2.2	18.2
PH11-11-15-14_14.FIN2	344	2.77	0.1699	0.0073	0.01599	0.00028	0.09	158.6	6.3	102.2	1.8	1052	97	DISC	DISC	35.6
PH11-11-15-14_15.FIN2	1253	3.34	0.1146	0.0034	0.01567	0.0002	0.19	110	3.1	100.2	1.3	307	63	100.2	1.3	8.9
PH11-11-15-14_16.FIN2	353.9	2.91	0.1129	0.0056	0.01512	0.00026	0.25	108.8	5.2	96.7	1.6	333	96	96.7	1.6	11.1
PH11-11-15-14_17.FIN2	723	4.20	0.1122	0.0047	0.01595	0.00025	0.20	107.7	4.2	102	1.6	230	83	102.0	1.6	5.3

PH11-11-15-14_19.FIN2	450	6.15	0.1279	0.0054	0.01585	0.00027	0.24	121.8	4.9	101.3	1.7	496	86	101.3	1.7	16.8
PH11-11-15-14_20.FIN2	313	3.47	0.1222	0.0059	0.01626	0.00032	0.04	116.6	5.3	103.9	2	340	100	103.9	2.0	10.9
PH11-11-15-14_21.FIN2	375.7	8.32	0.1239	0.0087	0.01578	0.00038	0.14	118.2	7.7	100.9	2.4	420	140	100.9	2.4	14.6
PH11-11-15-14_22.FIN2	65.5	-0.74	0.189	0.029	0.01644	0.00085	0.11	171	24	105.1	5.4	940	300	DISC	DISC	38.5
PH11-11-15-14_23.FIN2	356	3.96	0.1238	0.0063	0.01577	0.00024	0.09	117.9	5.7	100.9	1.5	420	100	100.9	1.5	14.4
PH11-11-15-14_24.FIN2	474	3.85	0.215	0.0086	0.01627	0.00025	0.32	196.8	7.2	104.1	1.6	1498	74	DISC	DISC	47.1
PH11-11-15-14_25.FIN2	410.1	1.64	0.1258	0.0072	0.01529	0.00034	0.20	119.9	6.4	97.8	2.1	540	120	97.8	2.1	18.4
PH11-11-15-14_26.FIN2	209.1	5.80	0.358	0.018	0.01801	0.00034	0.13	309	13	115	2.2	2198	90	DISC	DISC	62.8
PH11-11-15-14_27.FIN2	343.7	3.23	0.1241	0.0068	0.01526	0.00029	0.13	118.2	6.1	97.6	1.9	490	110	97.6	1.9	17.4
PH11-11-15-14_28.FIN2	630	15.80	0.1102	0.0046	0.01564	0.00027	0.02	105.8	4.2	100.1	1.7	220	84	100.1	1.7	5.4
PH11-11-15-14_29.FIN2	1610	1.55	0.1139	0.0027	0.01549	0.00017	0.09	109.7	2.5	99.09	1.1	335	54	99.1	1.1	9.7
PH11-11-15-14_30.FIN2	355	9.18	0.1249	0.0059	0.01604	0.0003	0.09	119	5.3	102.6	1.9	406	95	102.6	1.9	13.8
PH11-11-15-14_31.FIN2	581	3.09	0.1313	0.005	0.01691	0.00026	0.23	124.9	4.5	108.1	1.7	429	79	108.1	1.7	13.5
PH11-11-15-14_32.FIN2	1694	3.44	0.1122	0.0038	0.01535	0.00018	0.13	107.9	3.5	98.2	1.1	308	73	98.2	1.1	9.0
PH11-11-15-14_33.FIN2	1047	3.33	0.1102	0.0036	0.01586	0.00024	0.17	106	3.3	101.5	1.5	201	68	101.5	1.5	4.2
PH11-11-15-14_34.FIN2	403	3.18	0.1086	0.005	0.01597	0.00025	0.02	104.9	4.7	102.1	1.6	149	93	102.1	1.6	2.7
PH11-11-15-14_35.FIN2	1070	3.34	0.1128	0.0029	0.01657	0.0002	0.30	108.4	2.7	106	1.3	158	51	106.0	1.3	2.2
PH11-11-15-14_36.FIN2	845	4.71	0.1082	0.0034	0.01606	0.00024	0.22	104.1	3.1	102.7	1.5	135	64	102.7	1.5	1.3
PH11-11-15-14_37.FIN2	832	5.20	0.1091	0.0037	0.01649	0.00024	0.19	105.3	3.3	105.4	1.5	108	67	105.4	1.5	0.1
PH11-11-15-14_38.FIN2	467	7.53	0.1274	0.0053	0.0162	0.00027	0.08	121.9	4.9	103.6	1.7	432	87	103.6	1.7	15.0
PH11-11-15-14_39.FIN2	193	9.75	0.123	0.013	0.01569	0.00037	0.74	115	10	100.3	2.4	300	140	100.3	2.4	12.8
PH11-11-15-14_40.FIN2	2314	11.31	0.1157	0.0047	0.0159	0.00034	0.45	111	4.3	101.7	2.2	280	75	101.7	2.2	8.4
PH11-11-15-14_41.FIN2	354	8.07	0.1056	0.0052	0.01553	0.00027	0.16	101.6	4.7	99.3	1.7	139	89	99.3	1.7	2.3
PH11-11-15-14_42.FIN2	567	3.38	0.1372	0.0056	0.01578	0.00026	0.39	130.2	5	100.9	1.6	644	86	100.9	1.6	22.5
PH11-11-15-14_43.FIN2	155	10.74	0.1071	0.0081	0.01567	0.00042	0.11	103.3	7.5	100.2	2.7	180	140	100.2	2.7	3.0
PH11-11-15-14_44.FIN2	460	8.07	0.1085	0.0073	0.01654	0.00038	0.19	103.8	6.7	105.8	2.4	80	120	105.8	2.4	1.9
PH11-11-15-14_45.FIN2	246.5	3.95	0.117	0.0066	0.0163	0.00032	0.21	111.6	6	104.2	2	250	110	104.2	2.0	6.6

Table S2. Whole-rock major and trace element geochemistry results.

Sample name	PH-11-10-15-16	PH-11-11-15-1	PH-11-10-15-19	PH-11-11-15-14	PH-11-11-15-2
Rock type	migmatitic orthogneiss	migmatitic orthogneiss	migmatitic orthogneiss	leucogranite	foliated granitoid
Location	28° 46' 37.35329"N 95° 53' 0.48016"E	28° 47' 16.87722"N 95° 54' 32.55811"E	28° 48' 52.81091"N 95° 55' 17.15657"E	28° 31' 52.25188"N 95° 50' 39.58413"E	28° 36' 12.17412"N 95° 51' 24.98038"E
Major oxides (wt %)					
SiO_2	67.80	58.70	74.34	67.67	71.72
Al_2O_3	15.44	18.05	14.70	16.38	15.27
$Fe_2O_3(T)$	4.41	6.40	1.29	2.37	2.24
MnO	0.07	0.10	0.02	0.05	0.03
MgO	1.17	2.35	0.16	0.59	0.53
CaO	3.77	6.40	1.95	3.28	2.31
Na_2O	4.46	4.16	5.49	5.12	5.08
K_2O	0.98	0.99	0.92	2.21	1.24
TiO_2	0.45	0.67	0.05	0.19	0.25
P_20_5	0.11	0.09	0.01	0.03	0.01
LOI	1.21	2.34	1.69	1.93	1.57
Total	99.87	100.30	100.60	99.82	100.20
Trace elements (ppm)					
Sc	5.00	17.00	1.00	4.00	1.00
Be	2.00	1.00	2.00	1.00	< 1
V	55.00	138.00	9.00	34.00	27.00
Cr	< 20	40.00	< 20	< 20	< 20
Co	7.00	14.00	< 1	3.00	3.00
Ni	< 20	20.00	< 20	< 20	< 20
Cu	850.00	50.00	20.00	10.00	70.00
Zn	90.00	80.00	< 30	50.00	40.00
Ga	18.00	20.00	17.00	19.00	11.00
Ge	1.00	1.00	1.00	< 1	< 1
As	< 5	< 5	< 5	< 5	< 5
Rb	18.00	20.00	17.00	54.00	21.00
Sr	405.00	591.00	380.00	797.00	434.00
Y	17.00	15.00	3.00	3.00	1.00
Zr	109.00	73.00	21.00	61.00	29.00
Nb	4.00	2.00	1.00	2.00	1.00
Mo	< 2	< 2	< 2	< 2	< 2
Ag	0.80	0.70	0.50	0.50	0.50
In	0.20	0.20	0.20	0.20	0.20
Sn	70.00	2.00	1.00	< 1	5.00
Sb	2.50	0.50	0.50	0.50	0.50
Cs	0.70	0.80	0.80	1.20	0.50
Ba	146.00	189.00	337.00	600.00	319.00
La	17.50	12.10	3.40	6.20	0.80
Ce	41.90	26.30	6.60	11.90	1.40
Pr	5.44	3.32	0.79	1.35	0.16
Nd	22.10	13.60	3.20	5.20	0.70
Sm	4.70	3.20	0.80	0.90	0.20
Eu	1.06	0.99	0.47	0.28	0.19
Gd	4.10	3.40	0.70	0.80	0.20
Tb	0.60	0.50	0.10	0.10	0.10
Dy	3.40	3.10	0.50	0.60	0.20
Ho	0.60	0.60	0.10	0.10	0.10
Er	1.60	1.80	0.30	0.30	0.10
Tm	0.25	0.27	0.05	< 0.05	0.05
Yb	1.60	1.70	0.30	0.30	0.20
Lu	0.26	0.26	0.05	0.06	0.01
Hf	3.40	2.20	0.90	1.90	0.60
Ta	0.20	0.10	0.10	0.20	0.10
W	1.00	1.00	1.00	1.00	1.00
Tl	0.30	0.30	0.30	0.40	0.20
Pb	83.00	10.00	16.00	21.00	10.00
Bi	0.40	0.40	0.40	0.40	0.40
Th	1.80	2.50	1.40	1.40	0.10
U	0.40	0.40	0.30	0.40	0.10
Ti	2678.60	3970.70	306.80	1126.90	1451.40

Table S3. Analytical details of $^{40}Ar/^{39}Ar$ thermochronology for samples PH-11-9-15-36, PH-1-8-13-22, PH-1-15-20-6, and PH-11-10-15-19.

step	T (C)	t (min.)	^{36}Ar	^{37}Ar	^{38}Ar	^{39}Ar	^{40}Ar	$\%^{40}Ar^*$	% ^{39}Ar rlsd	Ca/K	$^{40}Ar^*/^{39}ArK$	Age (Ma)	1s.d.
Sample PH-11-9-15-36, Muscovite, 25.15 mg, J = 0.001672 ± 0.54%													
4 amu discrimination = 0.7814 ± 0.09%, $^{40}/^{39}K$ = 0.132 ± 4.62%, $^{36}/^{37}Ca$ = 0.000211 ± 0.78%, $^{39}/^{37}Ca$ = 0.000632 ± 0.57%													
1	810	12	1.581	0.257	0.969	46.747	838.841	28.1	1.5	0.040765	4.685384	14.08	0.20
2	870	12	0.538	0.190	0.672	43.897	495.178	58.3	1.4	0.032094	6.076241	18.24	0.17
3	900	12	0.198	0.098	0.610	47.182	412.302	81.3	1.5	0.015401	6.547611	19.64	0.12
4	930	12	0.659	0.098	1.952	149.991	1420.32	81.3	4.7	0.004845	7.162586	21.48	0.22
5	960	12	1.359	0.196	8.807	692.706	5593.04	89.2	21.7	0.002098	6.718561	20.15	0.11
6	990	12	0.402	0.142	5.126	412.722	3152.95	93.5	12.9	0.002551	6.660567	19.98	0.11
7	1020	12	0.375	0.116	3.175	250.943	1945.70	91.1	7.9	0.003428	6.583138	19.75	0.11
8	1050	12	0.362	0.107	2.850	224.524	1754.58	90.7	7.0	0.003534	6.598221	19.79	0.11
9	1100	12	0.573	0.090	7.399	588.722	4403.55	93.3	18.5	0.001134	6.512087	19.54	0.11
10	1170	12	0.305	0.216	7.894	640.471	4796.41	95.8	20.1	0.002501	6.697106	20.09	0.11
11	1400	12	0.241	0.131	1.140	89.477	748.787	87.5	2.8	0.010856	6.767173	20.30	0.12
								Cumulative $\%^{39}Ar$ rlsd =	100.0		Total gas age =	19.89	0.03
										Steps 5–11	Wt. mean age =	19.9	0.1
											MSWD =	5.5	
Notes: isotope beams in mV, rlsd = released, error in age includes J error, all errors 1 sigma (^{36}Ar through ^{40}Ar are measured beam intensities, corrected for decay for the age calculations)													
Sample PH-1-8-13-22, Biotite, 17.62 mg, J = 0.001698 ± 0.46%													
4 amu discrimination = 0.7958 ± 0.03%, $^{40}/^{39}K$ = 0.132 ± 4.62%, $^{36}/^{37}Ca$ = 0.000211 ± 0.78%, $^{39}/^{37}Ca$ = 0.000632 ± 0.57%													
1	650	12	3.673	2.120	1.618	50.959	1790.71	23.7	6.4	0.422206	7.803614	23.75	0.31
2	700	12	1.245	0.937	1.040	58.616	923.331	49.7	7.4	0.162219	7.304032	22.24	0.16
3	750	12	0.301	0.437	0.974	71.695	653.162	82.4	9.0	0.061853	6.962402	21.20	0.11
4	800	12	0.151	0.289	0.785	60.060	499.671	88.5	7.5	0.048829	6.806190	20.73	0.13
5	850	12	0.158	0.208	0.549	40.357	351.613	83.6	5.1	0.052301	6.686664	20.37	0.17
6	900	12	0.190	0.691	0.682	52.459	467.537	84.8	6.6	0.13367	6.979248	21.25	0.15
7	950	12	0.206	2.447	0.741	56.348	478.674	84.5	7.1	0.440725	6.597860	20.10	0.15
8	1000	12	0.261	2.982	1.179	91.237	774.713	87.2	11.5	0.331693	6.863650	20.90	0.11
9	1060	12	0.176	0.724	1.687	131.863	1029.01	92.9	16.6	0.055716	6.739490	20.53	0.10
10	1120	12	0.131	1.342	1.650	129.525	979.805	94.3	16.3	0.105141	6.629220	20.19	0.10
11	1190	12	0.090	1.151	0.553	43.585	348.203	91.6	5.5	0.267997	6.617666	20.16	0.10
12	1400	12	0.082	0.467	0.122	8.797	121.548	83.8	1.1	0.538773	9.319463	28.33	0.16

								Cumulative %^{39}Ar rlsd =	100.0		Total gas age =	21.00	0.04
										Steps 3–11	Wt. mean age =	20.59	0.14
											MSWD =	13.5	
Notes: isotope beams in mV, rlsd = released, error in age includes J error, all errors 1 sigma													
(^{36}Ar through ^{40}Ar are measured beam intensities, corrected for decay for the age calculations)													
Sample PH-1-15-20-6 Muscovite, 3.70 mg, J = 0.0048 ± 0.51%													
4 amu discrimination = 1.0448 ± 0.03%, $^{40}/^{39}$K = 0.0113 ± 5.85%, $^{36}/^{37}$Ca = 0.000231 ± 0.25%, $^{39}/^{37}$Ca = 0.000655 ± 0.20%													
step	**T (C)**	**t (min.)**	**^{36}Ar**	**^{37}Ar**	**^{38}Ar**	**^{39}Ar**	**^{40}Ar**	**%^{40}Ar***	**% ^{39}Ar rlsd**	**Ca/K**	**^{40}Ar*/^{39}Ar K**	**Age (Ma)**	**1s.d.**
1	750	12	0.620	0.612	0.543	32.523	220.425	25.0	2.1	0.132758	1.386998	11.97	0.44
2	800	12	0.394	0.604	0.603	46.361	204.664	57.1	2.9	0.091913	2.020691	17.41	0.16
3	830	12	0.318	0.537	0.672	60.616	192.454	67.9	3.8	0.0625	2.034800	17.54	0.26
4	860	12	0.276	0.615	0.839	63.729	211.544	78.5	4.0	0.068082	2.105126	18.14	0.16
5	890	12	0.264	0.891	1.137	95.614	289.240	86.6	6.1	0.065743	2.257170	19.44	0.15
6	920	12	0.254	1.852	2.035	161.180	453.306	92.5	10.2	0.081063	2.381992	20.51	0.13
7	950	12	0.256	3.533	3.600	286.554	802.637	96.1	18.1	0.086982	2.555745	22.00	0.13
8	980	12	0.257	3.720	4.464	355.630	1005.33	96.8	22.5	0.073797	2.632325	22.65	0.15
9	1010	12	0.259	9.661	3.086	241.194	720.450	95.7	15.3	0.282601	2.641213	22.73	0.15
10	1040	12	0.233	24.176	1.867	143.982	457.024	95.8	9.1	1.184966	2.748828	23.65	0.16
11	1080	12	0.230	12.793	0.779	56.957	213.955	89.2	3.6	1.585274	2.625777	22.60	0.12
12	1120	12	0.226	9.676	0.372	23.826	126.722	78.3	1.5	2.86736	2.612914	22.49	0.46
13	1160	12	0.187	4.165	0.132	6.423	76.506	75.4	0.4	4.580641	3.393325	29.15	0.42
14	1220	12	0.305	10.239	0.101	3.650	97.013	19.6	0.2	19.90225	2.760997	23.75	0.88
15	1400	12	0.378	4.030	0.077	0.615	108.529	8.4	0.04	46.84557	5.425956	46.39	14.56
								Cumulative %^{39}Ar rlsd =	100.0		Total gas age =	21.50	0.12
										Steps 7–14	Wt. mean age =	22.8	0.4
											MSWD =	42.2	
Notes: isotope beams in mV, rlsd = released, error in age includes J error, all errors 1 sigma													
(^{36}Ar through ^{40}Ar are measured beam intensities, corrected for decay for the age calculations)													
Sample PH-11-10-15-19, Muscovite, 3.04 mg, J = 0.001655 ± 1.34%													
4 amu discrimination = 0.9819 ± 0.06%, $^{40}/^{39}$K = 0.132 ± 4.62%, $^{36}/^{37}$Ca = 0.000211 ± 0.78%, $^{39}/^{37}$Ca = 0.000632 ± 0.57%													
step	**T (C)**	**t (min.)**	**^{36}Ar**	**^{37}Ar**	**^{38}Ar**	**^{39}Ar**	**^{40}Ar**	**%^{40}Ar***	**% ^{39}Ar rlsd**	**Ca/K**	**^{40}Ar*/^{39}Ar K**	**Age (Ma)**	**1s.d.**
1	750	12	2.012	0.056	0.562	16.222	676.357	10.2	4.7	0.04685	4.178498	12.43	0.72
2	800	12	0.202	0.014	0.322	23.563	258.421	77.3	6.9	0.008063	8.181842	24.27	0.33
3	840	12	0.322	0.018	1.130	85.852	890.192	87.4	25.1	0.002845	8.113615	24.06	0.32
4	870	12	0.165	0.009	1.197	94.893	840.860	93.4	27.7	0.001287	8.155025	24.19	0.33
5	900	12	0.087	0.006	0.508	39.480	350.613	92.9	11.5	0.002063	8.024693	23.80	0.32
6	950	12	0.080	0.009	0.322	23.759	221.256	91.7	6.9	0.005141	8.159778	24.20	0.34

7	1020	12	0.165	0.024	0.288	20.046	215.809	79.4	5.9	0.016248	8.156723	24.19	0.33
8	1100	12	0.151	0.020	0.315	22.331	232.851	82.3	6.5	0.012155	8.157741	24.19	0.33
9	1180	12	0.067	0.015	0.137	10.694	110.373	88.1	3.1	0.019036	8.191687	24.29	0.34
10	1400	12	0.123	0.051	0.094	5.682	84.899	64.1	1.7	0.121817	7.841459	23.26	0.39
								Cumulative %^{39}Ar rlsd =	100.0		Total gas age =	23.55	0.07
										Steps 2–9	Wt. mean age =	24.1	0.1
											MSWD =	0.2	
Notes: isotope beams in mV, rlsd = released, error in age includes J error, all errors 1 sigma													
(^{36}Ar through ^{40}Ar are measured beam intensities, corrected for decay for the age calculations)													

Table S4. Analytical details of multi-domain diffusion $^{40}Ar/^{39}Ar$ thermochronology for sample PH-11-11-15-14.

	ID	Power	$^{40}Ar/^{39}Ar$	$^{37}Ar/^{39}Ar$	$^{36}Ar/^{39}Ar$	$^{39}Ar_K$	K/Ca	$^{40}Ar^*$	^{39}Ar	Age	±1s	Time
		(Watts)			(x 10^{-3})	(x 10^{-15} mol)		(%)	(%)	(Ma)	(Ma)	(min)
	PH-11-11-15-14, K-feldspar, 11.56 mg, J=0.0015357±0.02%, IC=0.9989127±0.0007362, NM-303F, Lab#=66864-01, Argus VI											
X	A	450.0	148.2	0.1238	457.9	1.0	4.1	8.7	1.0	35.9	1.0	10
X	B	450.0	12.09	0.0440	21.65	0.5	11.6	47.1	1.6	15.95	0.40	20
X	C	500.0	9.224	-0.0608	11.06	0.4	-	64.5	2.0	16.66	0.43	10
X	D	500.0	9.002	0.1232	9.420	1.1	4.1	69.2	3.2	17.43	0.17	20
X	E	550.0	8.702	0.0716	7.210	1.4	7.1	75.6	4.6	18.40	0.14	10
X	F	550.0	8.389	0.0982	6.294	1.3	5.2	77.9	6.1	18.29	0.14	20
X	G	600.0	8.012	0.0717	5.230	1.8	7.1	80.8	8.0	18.10	0.11	10
X	H	600.0	7.946	0.0414	4.497	1.8	12.3	83.3	9.9	18.52	0.11	20
X	I	650.0	7.609	0.0555	3.650	2.4	9.2	85.9	12.4	18.279	0.081	10
X	J	650.0	7.602	0.0310	3.350	2.7	16.5	87.0	15.3	18.501	0.074	20
X	K	700.0	7.614	0.0421	2.872	2.8	12.1	88.9	18.3	18.930	0.068	10
X	L	700.0	7.843	0.0484	2.822	3.0	10.5	89.4	21.5	19.609	0.068	20
X	M	750.0	8.049	0.0651	3.000	3.3	7.8	89.0	25.0	20.039	0.058	10
X	N	750.0	8.490	0.0536	2.958	3.7	9.5	89.8	29.0	21.297	0.057	20
X	O	800.0	9.312	0.0541	3.531	5.2	9.4	88.8	34.5	23.109	0.050	10
X	P	800.0	9.245	0.0331	2.655	7.3	15.4	91.5	42.3	23.636	0.038	20
X	Q	850.0	9.497	0.0535	2.221	12.2	9.5	93.1	55.3	24.697	0.026	10
X	R	850.0	9.428	0.0541	2.012	11.2	9.4	93.7	67.3	24.678	0.025	20
X	S	900.0	9.982	0.2217	2.338	7.0	2.3	93.3	74.9	25.987	0.038	10
X	T	900.0	10.07	0.1045	2.597	5.4	4.9	92.5	80.6	25.982	0.047	20
X	U	950.0	12.49	0.1380	3.896	2.8	3.7	90.9	83.6	31.638	0.089	10
X	V	950.0	13.58	0.1734	6.268	1.7	2.9	86.5	85.4	32.70	0.15	20
X	W	1000.0	15.20	0.2824	13.05	1.2	1.8	74.8	86.7	31.68	0.22	10
X	X	1000.0	14.75	0.1940	13.49	1.2	2.6	73.1	88.0	30.05	0.23	20
X	Y	1050.0	18.33	0.7617	16.08	1.0	0.67	74.4	89.1	37.97	0.28	10
X	Z	1050.0	20.70	0.3909	23.41	1.2	1.3	66.7	90.4	38.45	0.28	20
X	BA	1100.0	26.15	1.158	27.06	1.3	0.44	69.8	91.8	50.62	0.31	10
X	BB	1100.0	26.55	0.1924	29.59	2.1	2.7	67.1	94.1	49.44	0.22	20
X	BC	1100.0	29.31	0.1069	42.07	3.5	4.8	57.6	97.8	46.87	0.17	60
X	BD	1100.0	52.78	0.1070	117.9	2.0	4.8	34.0	100.0	49.80	0.36	120
	Integrated age ± 1s			n=30		93.5	4.5		K_2O=2.02%	26.020	0.020	

Notes:

Isotopic ratios were corrected for blank, radioactive decay, and mass discrimination, and not corrected for interfering reactions.

Errors quoted for individual analyses include analytical error only, without interfering reaction or J uncertainties.

Integrated age was calculated by summing the isotopic measurements of all steps.

Integrated age error was calculated by quadratically combining the errors of isotopic measurements of all steps.

Plateau age is the inverse-variance-weighted mean of selected steps.

Plateau age error is the inverse-variance-weighted mean error (Taylor, 1982) times root MSWD where MSWD >1.

Plateau error is the weighted error of Taylor (1982).

Isotopic abundances are from Steiger and Jäger (1977).

X preceding sample ID denotes the analyses excluded from plateau age calculations.

Weight percent K_2O is calculated from ^{39}Ar signal, sample weight, and instrument sensitivity.

Ages were calculated relative to the FC-2 Fish Canyon Tuff sanidine interlaboratory standard (28.201 Ma)
Decay Constant (LambdaK (total)) = 5.463e-10/a
Correction factors include:
$(^{39}Ar/^{37}Ar)_{Ca}$ = 0.0006926 ± 0.000016
$(^{36}Ar/^{37}Ar)_{Ca}$ = 0.0002702 ± 0.0000010
$(^{38}Ar/^{39}Ar)_{K}$ = 0.0121
$(^{40}Ar/^{39}Ar)_{K}$ = 0.000129 ± 8e-05

References

Steiger, R.H., Jäger, E., 1977, Subcommission on geochronology: convention on the use of decay constants in geo-and cosmochronology: Earth and Planetary Science Letters, v. 36, no. 3, p. 359-362.

Taylor, J.R., 1982, An Introduction to Error Analysis: The Study of Uncertainties in Physical Measurements, Univ. Sci. Books, Mill Valley, Calif., 270 p.

Table S5. Domain distribution details for $^{40}Ar/^{39}Ar$ thermochronology for sample PH-11-11-15-14.

Sample	PH-11-11-15-14 (kspar)
# of domains	6
log(D/r_1^2) /sec	10.198
volume fraction r_1	0.026
log(D/r_2^2) /sec	7.851
volume fraction r_2	0.053
log(D/r_3^2) /sec	5.254
volume fraction r_3	0.166
log(D/r_4^2) /sec	5.213
volume fraction r_4	0.406
log(D/r_5^2) /sec	5.196
volume fraction r_5	0.155
log(D/r_6^2) /sec	3.368
volume fraction r_6	0.195
E (kcal/mol)	46
log(D_o/r_o^2) /sec	7.2

Table S6. Electron backscatter diffraction analytical run conditions and processing variables.

Sample	PH-1-15-20-3	PH-1-15-20-5	PH-1-15-20-6	PH-1-15-20-8	PH-1-15-20-14
Stepsize	4.9 μm	9.8 μm	5.9 μm	5.9 μm	11.75 μm
Field width (mm)	6.79	5.04	11.9	6.52	11.4
Field height (mm)	1.28	1.56	4.49	3	3.23
Number of points	347648	313177	1481040	543000	267575
Hit rate	60.6%	50.9%	58.6%	81.2%	97.3%
Accelerating voltage	25 kV	25 kV	25 kV	25 kV	25 kV
Working distance	25.0 mm	25.0 mm	25.0 mm	25.0 mm	25.2 mm
Specimen tilt	70°	70°	70°	70°	70°
Binning mode	4 x 4	4 x 4	4 x 4	4 x 4	2 x 2
Exposure time	3.9	4.2	3.9	4.4	17.1
Hough resolution	60	60	60	60	100
Band detection mode	Edges	Edges	Edges	Edges	Edges
# of bands detected	8	8	8	8	12
Indexing mode	Optimized EBSD	Optimized EBSD	Optimized EBSD	Optimized EBSD	Optimized EBSD

Notes:
SEM: JEOL 7100FT
EBSD camera: Nordlys nano high-resolution detector
Acquisition software: Aztec 3.0